

## Rayleigh wave at imperfectly corrugated interface in FGPM structure

K. Hemalatha<sup>a</sup>, S. Kumar\* and A. Akshaya<sup>a</sup>

*Department of Mathematics, College of Engineering and Technology,  
SRM Institute of Science and Technology, Kattankulathur-603203, India*

*(Received March 16, 2023, Revised June 19, 2023, Accepted August 21, 2023)*

**Abstract.** The Rayleigh wave propagation is considered in the structure of the functionally graded piezoelectric material (FGPM) layer over the elastic substrate. The elastic substrate loosely bonds the layer through a corrugated interface, whereas its upper boundary is also corrugated but stress-free. Additionally, the solutions for the FGPM layer and substrate are derived using the fundamental variable separable approach to convert the partial differential equation to an ordinary differential equation. The results with boundary conditions lead to dispersion relations for the electrically open and electrically short cases in the determinant form. The outcomes have been numerically analyzed using a specific model. The findings were presented in the form of graphs, which were created using Mathematica 7. Graphs are plotted for variations in wavenumber and phase velocity. The outcomes may help measure interface defects and design Surface Acoustic Wave (SAW) devices.

**Keywords:** corrugation; functionally graded piezoelectric material; imperfect interface; Rayleigh wave

---

### 1. Introduction

FGPM (functionally graded piezoelectric materials) is used in signal transmission, information storage, and surface acoustic wave (SAW) devices. The fundamental characteristics of Love waves and their use in sensor devices were examined by Jakoby *et al.* (1997). Functionally gradient material plates stimulated by plane pressure wavelets were the subject of research by Liu *et al.* (1999) on elastic waves. Wu and Wu (2000) studied the impact of viscous liquid on the transmission of acoustic waves in piezoelectric materials. A study by Qian *et al.* (2004) investigated the effect of inhomogeneous initial stress on Love wave dispersion relations and phase velocities. Li *et al.* (2004) encountered the behavior of Love type waves in a multilayer, functionally graded piezoelectric structure. Jin *et al.* (2005) investigated the transmission behavior of surface waves in the presence of homogeneous and inhomogeneous initial stress in a piezoelectric medium. Several new studies (Du *et al.* 2007, Hua *et al.* 2007, Guo and Sun 2008, Cao *et al.* 2009) have been conducted on how Love waves move through a layered composite

---

\*Corresponding author, Assistant Professor, E-mail: santoshh@srmist.edu.in

<sup>a</sup>Research Scholar

FGPM system. In an FGPM layer coupled between a piezomagnetic plate and a pre-stressed piezoelectric half-space, Singhal *et al.* (2018) used the WKB approach to explore the propagation of a Love-type wave. It is continuous paragraph till Hemalatha *et al.* (2023).

Liu *et al.* (2019) examined the possibility of surface acoustic waves in a piezoelectric layer with a half-infinite elastic layer. In piezoelectric helical constructions, Liang *et al.* (2019) studied the dispersion characteristics of wave propagation. The Lamb waves of the FGPM on the pair stress theory were studied by Liu *et al.* (2021).

Surface acoustic waves, called Rayleigh waves, move along a solid's surface. They are commonly employed in non-destructive testing to find flaws. They can be created in materials in a variety of methods, for as by a localized impact or piezoelectric transduction. Rayleigh-type wave propagation was studied by Pal *et al.* (2015) in an anisotropic layer above a semi-infinite sandy substrate. Nonhomogeneous Magneto-Electro-Elastic half-spaces complex Rayleigh Waves were covered by Li *et al.* (2021). Saha *et al.* (2021) evaluated the influence of curved boundaries on the propagation properties of Rayleigh-type waves and SH-wave in a pre-stressing monoclinic media. Belyankova *et al.* (2021) investigated how Rayleigh waves propagated through structures with different types of FGPM coating. Rayleigh wave propagation in an FGPM layer on top of an elastic substrate was studied by Hemalatha *et al.* (2023).

The nature of seismic waves shown at the interface of different materials with various imperfections is the subject of ongoing research. Corrugated refers to a material or surface formed into a groove and a sequence of parallel ridges. Undulation affects the propagation of waves and vibrations via these structures. It leads to the investigation of the wave propagation effect of corrugated surfaces. The reflection and refraction of elastic waves at the corrugated boundary surface were discovered by the papers (Asano 1960, Asano 1961), Abubakar (1962), Bubakar (1962), Abubakar (1962). Dunkin and Eringen (1962) investigated the reflection of elastic waves from a half-space boundary. Asano (1966) came across the corrugated interface in the elastic waves medium. The reflection and refraction of SH waves at a corrugated interface between two heterogeneous half-space mediums were discussed by Salvin and Wolf (1970), Sumner and Dereisewicz (1972), Gupta (1987), Zhang and Shinozuka (1996), Tomar and Saini (1997), Tomar *et al.* (2002), Kumar *et al.* (2003), Tomar and Kaur (2003), Kaur *et al.* (2005), Tomar and Singh (2006, 2007). The corrugated interface between two distinct initially strained elastic half-spaces of qP-wave was discovered by Singh (2008). Singh (2011) investigated the corrugated interface of SH waves with elastic solid or viscoelastic half-spaces. The propagation of a Love wave in a corrugated isotropic layered media over a homogeneous isotropic half-space was studied by Singh (2011). Kundu (2014) studied the propagation of a Love wave across a porous half-space with irregularity in an initially stressed homogeneous layer. The influence of irregularity and heterogeneity on the stresses produced by an average moving load on a rough monoclinic half-space was investigated by Singh *et al.* (2014). The closed-form formulas of dispersion of Love wave propagation in imperfectly-bonded irregular layered FGPM structures were studied by Chaki and Singh (2020). Ray and Singh (2021) addressed how the corrugated interface's imperfections in piezoelectric-piezomagnetic composites affect plane wave reflection and refraction.

The stresses and displacements at the interface of two media are taken to be perfectly bonded earlier, which indicates that the stresses and displacements at the interface are the same. However, this concept is later generalized as an incomplete interface condition, implying that the displacement at the contact does not have to be continuous. The boundary conditions linked to stresses and displacements by equalities with transverse and average stiffness coefficients were established by Jones and Whittier (1967). At the loosely connected interface of the elastic

substrate, Murty (1975) discussed the one transverse condition for solving Stonley wave difficulties. The unsatisfactory boundary conditions between two solid elastic half-spaces were encountered by Lovrentyev and Rokhlin (1998).

With the belief that the layers within the earth are not homogeneous, i.e., uneven and loosely bonded, a study of Rayleigh wave propagation at corrugated and weakly bonded interfaces has been undertaken. An FGPM layer and elastic substrate make up a structure. A layer's material coefficient is exponentially graded. Moreover, the solutions for layer and substrate are obtained using the primary variable-separable method to reduce the partial differential equation to the ordinary one. The solutions with boundary conditions lead to dispersion relations in the determinant form of two cases: electrically open-circuit case (open case) and electrically short-circuit case (short case). The outcomes have been numerically analyzed using a specific model. The results were presented in graphs. The consequences of the study presented here find their application in the production and development of SAW devices. Understanding the mechanism behind the piezoelectric properties of various building components is essential for the successful application of piezoelectric materials for sustainable building development, but it also depends on keeping up with the most recent innovations and implementations in the building industry.

## Terminology

$\rho$	Mass density
$T_{ij}$	Stress tensor
$u_i$	mechanical displacement vector components
$D_i$	$i^{\text{th}}$ -directed electric displacements
$\rho_1$	mass density for layer
$\rho_2$	mass density for substrate
$C_{11}, C_{13}, C_{44}$	elastic constants
$e_{15}, e_{31}, e_{33}$	piezoelectric constants
$\kappa_{11}, \kappa_{33}$	dielectric constants
$S_{ij}$	strain tensor
$E_i$	elastic field intensity
$\varphi$	scalar electric potential function
$T_{11}^{(1)}, T_{13}^{(1)}, T_{33}^{(1)}$	stresses in the layer
$T_{11}^{(2)}, T_{13}^{(2)}, T_{33}^{(2)}$	elastic substrate stresses
$D_3^{(0)}$	vacuum electric displacements
$D_1^{(1)}, D_3^{(1)}$	layer electric displacements
$D_1^{(2)}, D_3^{(2)}$	elastic substrate electric displacements
$k \left( = \frac{2\pi}{\lambda} \right)$	wave number
$\lambda$	wavelength
$c$	phase velocity
$u_{11}, u_{31}$	layer's mechanical displacement components
$u_{12}, u_{32}$	elastic substrate's mechanical displacement components
$\varphi_0$	vacuum's electric potential function
$\varphi_1$	layer's electric potential function

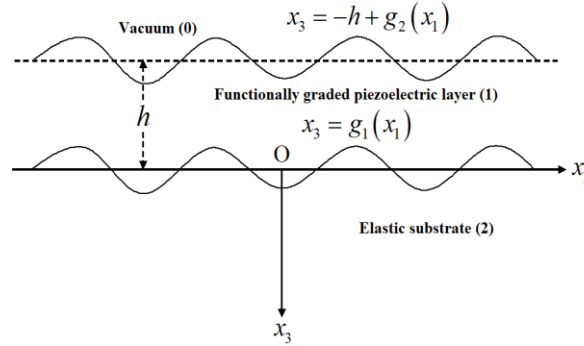


Fig. 1 Problem geometry

$\varphi_2$	elastic substrate's electric potential function
$\varepsilon_0$	vacuum's dielectric constant
$a, b$	corrugation amplitudes
$\alpha$	functional gradient parameter
$h$	thickness of the layer

## 2. Formulation of the problem

A multilayer piezoelectric design is depicted in Fig. 1. It comprises a transversely isotropic elastic substrate and a functionally graded,  $h$ -thickness transversely piezoelectric layer. It is thought that the layer's upper surface lacks traction.

The uppermost boundary surface of the layer is defined as  $x_3 = -h + g_2(x_1)$ , and the common interface of the layer and elastic substrate is  $g_1(x_1)$ , where  $g_1(x_1)$  and  $g_2(x_1)$  are continuous periodic functions of  $x_1$  and independent of  $x_2$ .

The definition of the Fourier series of  $g_1(x_1)$  and  $g_2(x_1)$  using an appropriate origin of coordinates is

$$g_l = \sum_{n=1}^{\infty} [g_n^{(l)} e^{in\lambda x_1} + g_{-n}^{(l)} e^{-in\lambda x_1}], l = 1, 2 \quad (1)$$

where  $n$  is the order of the series expansion  $g_n^{(l)}$  and  $g_{-n}^{(l)}$  are the Fourier expansions coefficients. The constants  $a, b, R_n^{(l)}, I_n^{(l)}$  will be introduced as follows

$$g_{\pm 1}^{(1)} = \frac{a}{2}, g_{\pm 1}^{(2)} = \frac{b}{2}, g_{\pm n}^{(l)} = \frac{R_n^{(l)} \mp I_n^{(l)}}{2}, l = 1, 2, n = 2, 3, \dots \quad (2)$$

and

$$\begin{aligned} g_1 &= a \cos \lambda x + R_2^{(1)} \cos 2\lambda x + I_2^{(1)} \sin n\lambda x + \dots \\ &+ R_n^{(1)} \cos 2\lambda x + I_n^{(1)} \sin n\lambda x + \dots, \\ g_2 &= b \cos \lambda x + R_2^{(2)} \cos 2\lambda x + I_2^{(2)} \sin n\lambda x + \dots \\ &+ R_n^{(2)} \cos 2\lambda x + I_n^{(2)} \sin n\lambda x + \dots, \end{aligned} \quad (3)$$

in which cosine but also sine Fourier coefficients are represented by  $R_n^{(l)}$  and  $I_n^{(l)}$  correspondingly. Cosine can be used to express the top and bottom boundary surfaces of the layer in the situation at hand, i.e.,  $g_1 = a \cos \lambda x$  and  $g_2 = b \cos \lambda x$ .

Governing equation in functionally graded materials

$$T_{ij,j} = \rho \ddot{u}_i, \quad (4)$$

$$D_{i,i} = 0 \quad (5)$$

where  $(i, j = 1, 2, 3)$  and the repeating index in the subscript denote summation, whereas the dot and comma stand for time differentiation but also space-coordinated differentiation, respectively.

The  $x_3$ -axis serves as the material's symmetric axis, and the constitutive relations for an isotropic material piezoelectric medium are

$$\begin{bmatrix} T_{11} \\ T_{22} \\ T_{33} \\ T_{23} \\ T_{31} \\ T_{12} \end{bmatrix} = \begin{bmatrix} C_{11} & C_{12} & C_{13} & 0 & 0 & 0 \\ C_{12} & C_{11} & C_{13} & 0 & 0 & 0 \\ C_{13} & C_{13} & C_{33} & 0 & 0 & 0 \\ 0 & 0 & 0 & C_{44} & 0 & 0 \\ 0 & 0 & 0 & 0 & C_{44} & 0 \\ 0 & 0 & 0 & 0 & 0 & C_{66} \end{bmatrix} \begin{bmatrix} S_{11} \\ S_{22} \\ S_{33} \\ S_{23} \\ S_{31} \\ S_{12} \end{bmatrix} - \begin{bmatrix} 0 & 0 & e_{13} \\ 0 & 0 & e_{31} \\ 0 & 0 & e_{33} \\ 0 & e_{15} & 0 \\ e_{15} & 0 & 0 \\ 0 & 0 & 0 \end{bmatrix} \begin{bmatrix} E_1 \\ E_2 \\ E_3 \end{bmatrix}, \quad (6)$$

$$\begin{bmatrix} D_1 \\ D_2 \\ D_3 \end{bmatrix} = \begin{bmatrix} 0 & 0 & 0 & 0 & e_{15} & 0 \\ 0 & 0 & 0 & e_{15} & 0 & 0 \\ e_{31} & e_{31} & e_{33} & 0 & 0 & 0 \end{bmatrix} \begin{bmatrix} S_{11} \\ S_{22} \\ S_{33} \\ S_{23} \\ S_{31} \\ S_{12} \end{bmatrix} + \begin{bmatrix} \kappa_{11} & 0 & 0 \\ 0 & \kappa_{11} & 0 \\ 0 & 0 & \kappa_{33} \end{bmatrix} \begin{bmatrix} E_1 \\ E_2 \\ E_3 \end{bmatrix}, \quad (7)$$

Expressions (6) and (7)'s  $S_{ij}$  and  $E_i$  were defined by the following expression

$$\begin{aligned} S_{11} &= \frac{\partial u_1}{\partial x_1}, S_{22} = \frac{\partial u_2}{\partial x_2}, S_{33} = \frac{\partial u_3}{\partial x_3}, \\ S_{23} &= \frac{\partial u_3}{\partial x_2} + \frac{\partial u_2}{\partial x_3}, S_{31} = \frac{\partial u_1}{\partial x_3} + \frac{\partial u_3}{\partial x_1}, \\ S_{12} &= \frac{\partial u_1}{\partial x_2} + \frac{\partial u_2}{\partial x_1}, \end{aligned} \quad (8)$$

$$E_1 = -\frac{\partial \varphi}{\partial x_1}, E_2 = -\frac{\partial \varphi}{\partial x_2}, E_3 = -\frac{\partial \varphi}{\partial x_3}, \quad (9)$$

It is assumed that the Rayleigh wave propagation is in the positive direction of the  $x_1$ -axis, and the mechanical displacement components and  $\varphi$  are as follows

$$\begin{aligned} u_1 &= u_1(x_1, x_3, t), u_2 = 0, \\ u_3 &= u_3(x_1, x_3, t), \varphi = \varphi(x_1, x_3, t), \end{aligned} \quad (10)$$

and independent of  $x_2$ -coordinate, i.e.,  $\frac{\partial}{\partial x_2} \equiv 0$ .

To differentiate stress components and the electric displacements of the layer, the substrate and

the vacuum, the superscript as index “1”, the superscript as index “2”, and the superscript as index “0” are used for the piezoelectric layer, elastic substrate, and vacuum, respectively. To differentiate the elastic, piezoelectric and dielectric constants of the layer, and the substrate, the superscript as index “(10)”, the superscript as index “(20)” are used for the functionally graded piezoelectric layer, and elastic substrate, respectively. Henceforth, for sake of clarity,  $u_{ij}$  is the mechanical displacement components, “ $i$ ” represents direction of displacement component and “ $j$ ” represents the medium.

### 3. The problem’s solution

#### 3.1 FGPM layer solution

By changing conditions (8)-(10), Eqs. (6) and (7), and the equations of motion on Rayleigh wave propagation for a FGPM layer, Eqs. (4) and (5)

$$\frac{\partial T_{11}^{(1)}}{\partial x_1} + \frac{\partial T_{13}^{(1)}}{\partial x_3} = \rho_1 \frac{\partial^2 u_{11}}{\partial t^2}, \quad (11)$$

$$\frac{\partial T_{31}^{(1)}}{\partial x_1} + \frac{\partial T_{33}^{(1)}}{\partial x_3} = \rho_1 \frac{\partial^2 u_{31}}{\partial t^2}, \quad (12)$$

$$\frac{\partial D_1^{(1)}}{\partial x_1} + \frac{\partial D_3^{(1)}}{\partial x_3} = 0, \quad (13)$$

In terms of  $u_i$  and  $\varphi_i$ ,  $T_{ij}$  and  $D_i$  is defined as

$$\begin{aligned} T_{11}^{(1)} &= C_{11}^{(1)} \frac{\partial u_{11}}{\partial x_1} + C_{13}^{(1)} \frac{\partial u_{31}}{\partial x_3} + e_{31}^{(1)} \frac{\partial \varphi_1}{\partial x_3}, \\ T_{33}^{(1)} &= C_{13}^{(1)} \frac{\partial u_{11}}{\partial x_1} + C_{33}^{(1)} \frac{\partial u_{31}}{\partial x_3} + e_{33}^{(1)} \frac{\partial \varphi_1}{\partial x_3}, \\ T_{13}^{(1)} &= C_{44}^{(1)} \left( \frac{\partial u_{11}}{\partial x_3} + \frac{\partial u_{31}}{\partial x_1} \right) + e_{15}^{(1)} \frac{\partial \varphi_1}{\partial x_1}, \end{aligned} \quad (14)$$

$$\begin{aligned} D_1^{(1)} &= e_{15}^{(1)} \left( \frac{\partial u_{11}}{\partial x_3} + \frac{\partial u_{31}}{\partial x_1} \right) - \kappa_{11}^{(1)} \frac{\partial \varphi_1}{\partial x_1}, \\ D_3^{(1)} &= e_{31}^{(1)} \frac{\partial u_{11}}{\partial x_1} + e_{33}^{(1)} \frac{\partial u_{31}}{\partial x_3} - \kappa_{33}^{(1)} \frac{\partial \varphi_1}{\partial x_3}, \end{aligned} \quad (15)$$

The hypothesis is that the material constants change exponentially with thickness, i.e.

$$\begin{aligned} C_{ij}^{(1)}(x_3) &= C_{ij}^{(10)} e^{\alpha x_3}, e_{ij}^{(1)}(x_3) = e_{ij}^{(10)} e^{\alpha x_3}, \\ \kappa_{ij}^{(1)}(x_3) &= \kappa_{ij}^{(10)} e^{\alpha x_3}, \rho_1 = \rho_{10} e^{\alpha x_3}. \end{aligned} \quad (16)$$

Eqs. (14)-(16) are substituted into Eqs. (11)-(13) to yield

$$\begin{aligned}
& C_{11}^{(10)} \frac{\partial^2 u_{11}}{\partial x_1^2} + C_{13}^{(10)} \frac{\partial^2 u_{31}}{\partial x_1 \partial x_3} + e_{31}^{(10)} \frac{\partial^2 \varphi_1}{\partial x_1 \partial x_3} \\
& + C_{44}^{(10)} \left( \frac{\partial^2 u_{11}}{\partial x_3^2} + \frac{\partial^2 u_{31}}{\partial x_1 \partial x_3} \right) + e_{15}^{(10)} \frac{\partial^2 \varphi_1}{\partial x_1 \partial x_3} \\
& + \alpha C_{44}^{(10)} \left( \frac{\partial u_{11}}{\partial x_3} + \frac{\partial u_{31}}{\partial x_1} \right) + \alpha e_{15}^{(10)} \frac{\partial \varphi_1}{\partial x_1} = \rho_{10} \frac{\partial^2 u_{11}}{\partial t^2},
\end{aligned} \tag{17}$$

$$\begin{aligned}
& C_{44}^{(10)} \left( \frac{\partial^2 u_{11}}{\partial x_1 \partial x_3} + \frac{\partial^2 u_{31}}{\partial x_1^2} \right) + e_{15}^{(10)} \frac{\partial^2 \varphi_1}{\partial x_1^2} + C_{13}^{(10)} \frac{\partial^2 u_{11}}{\partial x_1 \partial x_3} \\
& + C_{33}^{(10)} \frac{\partial^2 u_{31}}{\partial x_3^2} + e_{33}^{(10)} \frac{\partial^2 \varphi_1}{\partial x_3^2} + \alpha C_{13}^{(10)} \frac{\partial u_{11}}{\partial x_1} \\
& + \alpha C_{33}^{(10)} \frac{\partial u_{31}}{\partial x_3} + \alpha e_{33}^{(10)} \frac{\partial \varphi_1}{\partial x_3} = \rho_{10} \frac{\partial^2 u_{31}}{\partial t^2},
\end{aligned} \tag{18}$$

$$\begin{aligned}
& e_{15}^{(10)} \left( \frac{\partial^2 u_{11}}{\partial x_1 \partial x_3} + \frac{\partial^2 u_{31}}{\partial x_1^2} \right) - \kappa_{11}^{(10)} \frac{\partial^2 \varphi_1}{\partial x_1^2} + e_{31}^{(10)} \frac{\partial^2 u_{11}}{\partial x_1 \partial x_3} \\
& + e_{33}^{(10)} \frac{\partial^2 u_{31}}{\partial x_3^2} - \kappa_{33}^{(10)} \frac{\partial^2 \varphi_1}{\partial x_3^2} + \alpha e_{31}^{(10)} \frac{\partial u_{11}}{\partial x_1} \\
& + \alpha e_{33}^{(10)} \frac{\partial u_{31}}{\partial x_3} - \alpha \kappa_{33}^{(10)} \frac{\partial \varphi_1}{\partial x_3} = 0,
\end{aligned} \tag{19}$$

Eqs. (17)-(19) are considered to have the following solutions

$$\{u_{11}, u_{31}, \varphi_1\}(x_1, x_3, t) = \{U_{11}, U_{31}, \Phi_1\}(x_3) e^{ik(x_1 - ct)}, \tag{20}$$

where, the unidentified functions  $U_{11}$ ,  $U_{31}$  and  $\Phi_1$  are engaged.

Calculations (17), (18), as well as (19) are changed to Eq. (20) purpose of providing

$$\begin{aligned}
& C_{44}^{(10)} \frac{d^2 U_{11}}{dx_3^2} + \alpha C_{44}^{(10)} \frac{dU_{11}}{dx_3} + (\rho_{10} k^2 c^2 - C_{11}^{(10)} k^2) U_{11} \\
& + (ik) \left\{ (C_{13}^{(10)} + C_{44}^{(10)}) \frac{dU_{31}}{dx_3} + \alpha C_{44}^{(10)} U_{31} \right\} \\
& + (ik) \left\{ (e_{31}^{(10)} + e_{15}^{(10)}) \frac{d\Phi_1}{dx_3} + \alpha e_{15}^{(10)} \Phi_1 \right\} = 0,
\end{aligned} \tag{21}$$

$$\begin{aligned}
& (ik) \left\{ (C_{44}^{(10)} + C_{13}^{(10)}) \frac{dU_{11}}{dx_3} + \alpha C_{13}^{(10)} U_{11} \right\} \\
& + C_{33}^{(10)} \frac{d^2 U_{31}}{dx_3^2} + \alpha C_{33}^{(10)} \frac{dU_{31}}{dx_3} + (\rho_{10} k^2 c^2 - C_{44}^{(10)} k^2) U_{31} \\
& + e_{33}^{(10)} \frac{d^2 \Phi_1}{dx_3^2} + \alpha e_{33}^{(10)} \frac{d\Phi_1}{dx_3} - e_{15}^{(10)} k^2 \Phi_1 = 0,
\end{aligned} \tag{22}$$

$$\begin{aligned}
& -(ik) \left\{ \left( e_{15}^{(10)} + e_{31}^{(10)} \right) \frac{dU_{11}}{dx_3} + \alpha e_{31}^{(10)} U_{11} \right\} \\
& - e_{33}^{(10)} \frac{d^2 U_{31}}{dx_3^2} - \alpha e_{33}^{(10)} \frac{dU_{31}}{dx_3} + e_{15}^{(10)} k^2 U_{31} \\
& + \kappa_{33}^{(10)} \frac{d^2 \Phi_1}{dx_3^2} + \alpha \kappa_{33}^{(10)} \frac{d\Phi_1}{dx_3} - \kappa_{11}^{(10)} k^2 \Phi_1 = 0,
\end{aligned} \tag{23}$$

The answers to Eqs. (21)-(23) can now be considered to be

$$\{U_{11}, U_{31}, \Phi_1\}(x_3) = \{A, B, C\}e^{-ksx_3}, \tag{24}$$

wherever unknown variables A, B and C are used.

Eq. (24) can be substituted for Eqs. (21)-(23) to produce

$$\begin{aligned}
& \left\{ C_{44}^{(10)} s^2 - \frac{\alpha}{k} C_{44}^{(10)} s + \left( \rho_{10} c^2 - C_{44}^{(10)} \right) \right\} A \\
& + (i) \left\{ - \left( C_{13}^{(10)} + C_{44}^{(10)} \right) s + \frac{\alpha}{k} C_{44}^{(10)} \right\} B \\
& + (i) \left\{ - \left( e_{31}^{(10)} + e_{15}^{(10)} \right) s + \frac{\alpha}{k} e_{15}^{(10)} \right\} C = 0,
\end{aligned} \tag{25}$$

$$\begin{aligned}
& (i) \left\{ - \left( C_{44}^{(10)} + C_{13}^{(10)} \right) s + \frac{\alpha}{k} C_{13}^{(10)} \right\} A \\
& + \left\{ C_{33}^{(10)} s^2 - \frac{\alpha}{k} C_{33}^{(10)} s + \left( \rho_{10} c^2 - C_{44}^{(10)} \right) \right\} B \\
& + \left\{ e_{33}^{(10)} s^2 - \frac{\alpha}{k} e_{33}^{(10)} s - e_{15}^{(10)} \right\} C = 0,
\end{aligned} \tag{26}$$

$$\begin{aligned}
& -(i) \left\{ \left( e_{15}^{(10)} + e_{31}^{(10)} \right) s + \frac{\alpha}{k} e_{31}^{(10)} \right\} A \\
& - \left\{ e_{33}^{(10)} s^2 - \frac{\alpha}{k} e_{33}^{(10)} s - e_{15}^{(10)} \right\} B \\
& + \left\{ \kappa_{33}^{(10)} s^2 - \frac{\alpha}{k} \kappa_{33}^{(10)} s - \kappa_{11}^{(10)} \right\} C = 0,
\end{aligned} \tag{27}$$

Eqs. (25)-(27) can be easily solved if the coefficient matrix's determinant is zero, that is

$$|a_{ij}| = 0, (i, j = 1, 2, 3) \tag{28}$$

where the coefficient of the preceding Eqs. (25)-(27) as defined in Appendix A is  $a_{ij}$  ( $i, j = 1, 2, 3$ ).

The preceding algebraic expression with order 6 in  $s$  results from expanding Eq. (28).

$$a_0 s^6 + a_1 s^5 + a_2 s^4 + a_3 s^3 + a_4 s^2 + a_5 s + a_6 = 0, \tag{29}$$

there, according to Appendix B,  $a_i$  ( $i = 0, 1, \dots, 6$ ).

Let the roots of a components  $U_{31j}$ ,  $U_{11j}$  and  $U_{11j}$ ,  $\Phi_{1j}$  equivalent to  $s = s_j$  be  $s_j$  ( $j = 1, \dots, 6$ ),

$$\frac{U_{31j}}{U_{11j}} = \frac{B_j}{A_j} = \frac{a_{13j} a_{21j} - a_{11j} a_{23j}}{a_{12j} a_{23j} - a_{13j} a_{22j}} = \delta_{1j}, \tag{30}$$

$$\frac{\Phi_{1j}}{U_{11j}} = \frac{C_j}{A_j} = \frac{a_{11j} a_{22j} - a_{12j} a_{21j}}{a_{12j} a_{23j} - a_{13j} a_{22j}} = \gamma_{1j}, \tag{31}$$

wherever,  $a_{ijk}$  ( $i, j = 1, 2, 3; k=1, 2, \dots, 6$ ) as specified in Appendix C.

As a result, the final formulation for Eqs. (17)-(19) is

$$\begin{aligned} u_{11}(x_1, x_3, t) &= \sum_{j=1}^6 A_j e^{[-ks_j x_3 + ik(x_1 - ct)]}, \\ u_{31}(x_1, x_3, t) &= \sum_{j=1}^6 \delta_{1j} A_j e^{[-ks_j x_3 + ik(x_1 - ct)]}, \\ \varphi_1(x_1, x_3, t) &= \sum_{j=1}^6 \gamma_{1j} A_j e^{[-ks_j x_3 + ik(x_1 - ct)]}, \end{aligned} \quad (32)$$

where the constants  $A_j$  are chosen at random.

### 3.2 Elastic substrate solution

The field equations for propagation of Rayleigh wave the elastic substrate can be obtained as

$$\frac{\partial T_{11}^{(2)}}{\partial x_1} + \frac{\partial T_{13}^{(2)}}{\partial x_3} = \rho_2 \frac{\partial^2 u_{12}}{\partial t^2}, \quad (33)$$

$$\frac{\partial T_{31}^{(2)}}{\partial x_1} + \frac{\partial T_{33}^{(2)}}{\partial x_3} = \rho_2 \frac{\partial^2 u_{32}}{\partial t^2}, \quad (34)$$

$$\frac{\partial D_1^{(2)}}{\partial x_1} + \frac{\partial D_3^{(2)}}{\partial x_3} = 0, \quad (35)$$

In terms of  $u_i$  and  $\varphi_i$ ,  $T_{ij}$  and  $D_i$  is defined as

$$\begin{aligned} T_{11}^{(2)} &= C_{11}^{(20)} \frac{\partial u_{12}}{\partial x_1} + C_{13}^{(20)} \frac{\partial u_{32}}{\partial x_3}, \\ T_{33}^{(2)} &= C_{13}^{(20)} \frac{\partial u_{12}}{\partial x_1} + C_{33}^{(20)} \frac{\partial u_{32}}{\partial x_3}, \\ T_{13}^{(2)} &= C_{44}^{(20)} \left( \frac{\partial u_{12}}{\partial x_3} + \frac{\partial u_{32}}{\partial x_1} \right), \end{aligned} \quad (36)$$

$$\begin{aligned} D_1^{(2)} &= -\kappa_{11}^{(20)} \frac{\partial \varphi_2}{\partial x_1}, \\ D_3^{(2)} &= -\kappa_{33}^{(20)} \frac{\partial \varphi_2}{\partial x_3}, \end{aligned} \quad (37)$$

Eqs. (36) and (37) are substituted into Eqs. (33)-(35) to yield

$$\begin{aligned} C_{11}^{(20)} \frac{\partial^2 u_{12}}{\partial x_1^2} + C_{13}^{(20)} \frac{\partial^2 u_{32}}{\partial x_1 \partial x_3} \\ + C_{44}^{(20)} \left( \frac{\partial^2 u_{12}}{\partial x_3^2} + \frac{\partial^2 u_{32}}{\partial x_1 \partial x_3} \right) = \rho_2 \frac{\partial^2 u_{12}}{\partial t^2}, \end{aligned} \quad (38)$$

$$C_{44}^{(20)} \left( \frac{\partial^2 u_{12}}{\partial x_1 \partial x_3} + \frac{\partial^2 u_{32}}{\partial x_1^2} \right) + C_{13}^{(20)} \frac{\partial^2 u_{12}}{\partial x_1 \partial x_3} + C_{33}^{(20)} \frac{\partial u_{32}}{\partial x_3} = \rho_2 \frac{\partial^2 u_{32}}{\partial t^2}, \quad (39)$$

$$\kappa_{11}^{(20)} \frac{\partial^2 \varphi_2}{\partial x_1^2} + \kappa_{33}^{(20)} \frac{\partial^2 \varphi_2}{\partial x_3^2} = 0, \quad (40)$$

Eqs. (38)-(40) are considered to have the following solutions

$$\{u_{12}, u_{32}, \varphi_2\}(x_1, x_3, t) = \{U_{12}, U_{32}, \Phi_2\}(x_3) e^{ik(x_1 - ct)}, \quad (41)$$

Eq. (41) can be substituted for Eqs. (38)-(40) to produce

$$C_{44}^{(20)} \frac{d^2 U_{12}}{dx_3^2} + (\rho_2 k^2 c^2 - C_{11}^{(20)} k^2) U_{12} + (ik) (C_{13}^{(20)} + C_{44}^{(20)}) \frac{dU_{32}}{dx_3} = 0, \quad (42)$$

$$C_{33}^{(20)} \frac{d^2 U_{32}}{dx_3^2} + (\rho_2 k^2 c^2 - C_{44}^{(20)} k^2) U_{32} + (ik) (C_{44}^{(20)} + C_{13}^{(20)}) \frac{dU_{12}}{dx_3} = 0, \quad (43)$$

$$\kappa_{33}^{(20)} \frac{d^2 \Phi_2}{dx_3^2} - \kappa_{11}^{(20)} k^2 \Phi_2 = 0, \quad (44)$$

From Eq. (44) can be written as

$$\frac{d^2 \Phi_2}{dx_3^2} - k^2 p^2 \Phi_2 = 0, \quad (45)$$

where  $p^2 = \frac{\kappa_{11}^{(20)}}{\kappa_{33}^{(20)}}$ .

The solution of the Eq. (45) is given by

$$\Phi_2(x_3) = (F_1 e^{-kp x_3} + F_2 e^{kp x_3}), \quad (46)$$

Now by Eq. (46) and considering that  $\varphi_2$  vanishes as  $x_3 \rightarrow -\infty$ , the solution of Eq. (40) is given by

$$\varphi_2(x_1, x_3, t) = F_1 e^{-kp x_3} e^{ik(x_1 - ct)}, \quad (47)$$

The answers to Eqs. (42) and (43) can now be considered to be

$$\{U_{12}, U_{32}\}(x_3) = \{G, H\} e^{-kq x_3}, \quad (48)$$

wherever unknown variables  $G$  and  $H$  are used.

Eq. (48) can be substituted for Eqs. (42) and (43) to produce

$$\{C_{44}^{(20)} q^2 + \rho_2 c^2 - C_{11}^{(20)}\} G + \{(-iq) (C_{13}^{(20)} + C_{44}^{(20)})\} H = 0, \quad (49)$$

$$\left\{-(iq)\left(C_{44}^{(20)} + C_{13}^{(20)}\right)\right\}G + \left\{C_{33}^{(20)}q^2 + \rho_2c^2 - C_{44}^{(20)}\right\}H = 0, \quad (50)$$

Eqs. (49) and (50) can be easily solved if the coefficient matrix's determinant is zero, that is

$$|b_{ij}| = 0, (i, j = 1, 2) \quad (51)$$

where the coefficient of preceding Eqs. (49) and (50) above, given in Appendix D, is  $b_{ij}(i, j = 1, 2)$ .

The preceding algebraic expression with order 4 in  $q$  results from expanding Eq. (51).

$$b_0q^4 + b_1q^2 + b_2 = 0, \quad (52)$$

there, according to Appendix E,  $b_i(i = 0, 1, 2)$ .

Considering that  $\pm q_1, \pm q_2$  are roots of Eq. (52) and displacements are provided as

$$\begin{aligned} U_{12}(x_3) &= G_1e^{-kq_1x_3} + G_2e^{-kq_2x_3} \\ &+ G_3e^{kq_3x_3} + G_4e^{kq_4x_3}, \\ U_{32}(x_3) &= \delta_{21}G_1e^{-kq_1x_3} + \delta_{22}G_2e^{-kq_2x_3} \\ &- \delta_{21}G_3e^{kq_3x_3} - \delta_{22}G_4e^{kq_4x_3}, \end{aligned} \quad (53)$$

$$\text{where } q_1^2 = \frac{-b_1 - \sqrt{b_1^2 - 4b_0b_2}}{2b_0}, \text{ and } q_2^2 = \frac{-b_1 + \sqrt{b_1^2 - 4b_0b_2}}{2b_0}.$$

The roots of components  $U_{32j}, U_{12j}$  related to  $q = q_j$  are given by  $q_j(j = 1, 2)$ .

$$\frac{U_{32j}}{U_{12j}} = \frac{H_j}{G_j} = \frac{b_{11j}}{b_{12j}} = \delta_{2j}, \quad (54)$$

wherever,  $b_{ijk}(i, j, k=1, 2)$  defined in Appendix F.

Eq. (53) is approximate answer to substrate can be expressed as

$$\begin{aligned} U_{12}(x_3) &= G_1e^{-kq_1x_3} + G_2e^{-kq_2x_3} \\ U_{32}(x_3) &= \delta_{21}G_1e^{-kq_1x_3} + \delta_{22}G_2e^{-kq_2x_3}, \end{aligned} \quad (55)$$

As a result, the final formulation of Eqs. (38)-(40) is

$$\begin{aligned} u_{12}(x_1, x_3, t) &= \sum_{j=1}^2 G_j e^{[-kq_jx_3 + ik(x_1 - ct)]}, \\ u_{32}(x_1, x_3, t) &= \sum_{j=1}^2 \delta_{2j} G_j e^{[-kq_jx_3 + ik(x_1 - ct)]}, \end{aligned} \quad (56)$$

$G_j$ 's were random constants in this situation.

### 3.3 Vacuum solution

Compared to the piezoelectric medium,  $\varepsilon_0$  of air is smaller than layer. As a result, the air is assumed to be a vacuum, and  $\varphi_0(x_3 < -h)$  of air fulfills the Laplace equation, that is

$$\frac{\partial^2 \varphi_0}{\partial x_1^2} + \frac{\partial^2 \varphi_0}{\partial x_3^2} = 0, \quad (57)$$

Taking into account that  $\varphi_0$  disappears as  $x_3 \rightarrow -\infty$ , the answer to Eq. (57) is obtained by

$$\varphi_0 = A_0 e^{kx_3} e^{ik(x_1 - ct)}, \quad (58)$$

where  $A_0$  is an undefined constant.

Electric vacuum displacement is

$$D_3^{(0)} = -\varepsilon_0 \frac{\partial \varphi_0}{\partial x_3}. \quad (59)$$

#### 4. Boundary conditions

The layer has been loosely bonded with elastic substrate and have corrugated interface where as upper boundary as stress free and corrugated. Additionally, it is thought that the top border is an electrically open case as well as a electrically short case. At the interface, scalar potential and electrical displacement are continuous functions. These conditions are illustrated mathematically below,

1. The mechanical traction free condition at  $x_3 = -h + g_2(x_1)$  are

$$\begin{aligned} T_{33}^{(1)} - g_2' T_{13}^{(1)} &= 0, \\ T_{13}^{(1)} - g_2' T_{11}^{(1)} &= 0, \end{aligned} \quad (60)$$

2. The electrically boundary condition at  $x_3 = -h + g_2(x_1)$  are

a) Electrically open case

$$\begin{aligned} \varphi_1 &= \varphi_0, \\ D_3^{(1)} &= D_3^{(0)}, \end{aligned} \quad (61)$$

b) Electrically short case

$$\varphi_1 = 0, \quad (62)$$

3. The continuous condition at  $x_3 = g_1(x_1)$  are

$$\begin{aligned} T_{33}^{(2)} - g_1' T_{13}^{(2)} &= K_n(u_{31} - u_{32}), \\ T_{31}^{(2)} - g_1' T_{11}^{(2)} &= K_t(u_{11} - u_{12}), \\ T_{33}^{(2)} - g_1' T_{13}^{(2)} &= T_{33}^{(1)} - g_1' T_{13}^{(1)}, \\ T_{31}^{(2)} - g_1' T_{13}^{(2)} &= T_{31}^{(1)} - g_1' T_{13}^{(1)}, \\ \varphi_1 &= \varphi_2, \\ D_3^{(1)} &= D_3^{(2)}, \end{aligned} \quad (63)$$

where  $K_n$  and  $K_t$  are normal and transverse stiffness coefficients of a unit layer thickness and have the dimension  $\text{N/m}^3$ .

#### 5. Dispersion relations

In this instance, two cases are taken into consideration: an electrically open as well as a short

case.

### 5.1 Electrically open case

Yielding the solutions of layer, elastic substrate, and vacuum and their related stress and electric components into boundary conditions (60), (61), and (63), we get the homogeneous equations of unknown constants  $A_0, A_j's, G_j's$  and  $F_1$ .

From that equations eliminating the  $A_0, A_j's, G_j's$  and  $F_1$ , We obtain the dispersion relation in tenth-order determinant form for a piezoelectric layer covering a elastic substrate that is subject to the top boundary condition of a free surface.

$$|m_{xy}| = 0, \quad (64)$$

for every  $x, y = 1, 2, \dots, 10$  and  $m_{xy}$  as described in Appendix G.

### 5.2 Electrically short case

Yielding the solutions of layer, elastic substrate, and their related stress and electric components into boundary conditions (60), (62), and (63), we get the homogeneous equations of unknown constants  $A_j's, G_j's$  and  $F_1$ .

From that equations eliminating the constants  $A_j's, G_j's$  and  $F_1$ , We obtain the dispersion relation in tenth-order determinant form for a piezoelectric layer covering an elastic substrate that is subject to the top boundary condition of a free surface.

$$|n_{xy}| = 0, \quad (65)$$

for every  $x, y = 1, 2, \dots, 9$  and  $n_{xy}$  as described in Appendix H.

## 6. Numerical calculations and graphical discussions

The following information has been taken into account for the execution of numerical computation as well as a graphic illustration of the phase velocity of the Rayleigh wave propagation in a corrugated FGPM layer imperfectly bonded to elastic substrate:

(i) For FGPM layer

$$\begin{aligned} C_{11}^{(10)} &= 151 \times 10^9 \text{ Pa}, C_{13}^{(10)} = 96 \times 10^9 \text{ Pa}, C_{33}^{(10)} = 124 \times 10^9 \text{ Pa}, \\ C_{44}^{(10)} &= 23 \times 10^9 \text{ Pa}, e_{31}^{(10)} = -5.1 \text{ C/m}^2, e_{33}^{(10)} = 27 \text{ C/m}^2, \\ e_{15}^{(10)} &= 17 \text{ C/m}^2, \rho_1 = 7500 \text{ Kg/m}^3, \kappa_{11}^{(10)} = 15 \times 10^{-9} \text{ C/Vm}, \\ \kappa_{33}^{(10)} &= 13.27 \times 10^{-9} \text{ C/Vm}. \end{aligned}$$

(ii) For elastic substrate:

$$\begin{aligned} C_{11}^{(20)} &= 226 \times 10^9 \text{ Pa}, C_{13}^{(20)} = 121 \times 10^9 \text{ Pa}, C_{33}^{(20)} = 218 \times 10^9 \text{ Pa}, \\ C_{44}^{(20)} &= 48 \times 10^9 \text{ Pa}, \rho_2 = 7500 \text{ Kg/m}^3, \kappa_{11}^{(20)} = 0.19 \times 10^{-9} \text{ C/Vm}, \\ \kappa_{33}^{(20)} &= 5.1 \times 10^{-9} \text{ C/Vm}. \end{aligned}$$

Vacuum dielectric constant  $\epsilon_0 = 8.85 \times 10^{-12} \text{ F/m}$ .

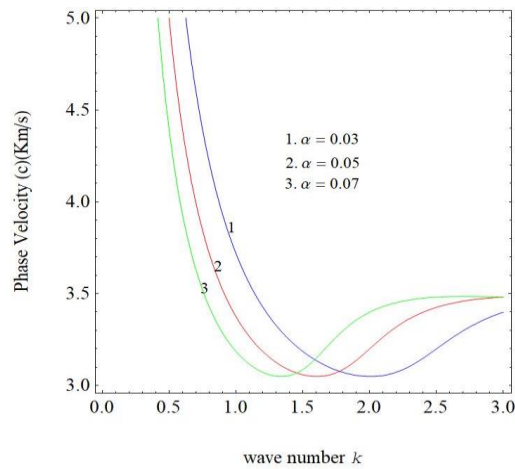


Fig. 2 Wave number versus phase velocity for various values of  $\alpha$ : electrically open case

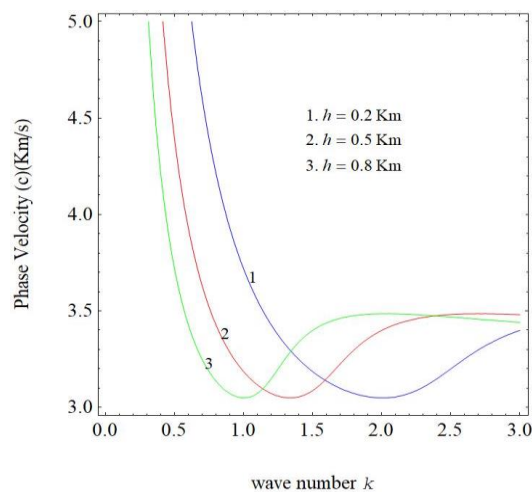


Fig. 3 Wave number versus phase velocity for various values of  $h$ : electrically open case

Now, to execute the numerical results and plot the graphs, a particular case of corrugation has been considered i.e.,  $g_1 = a \cos \lambda x$ , and  $g_2 = b \cos \lambda x$ .

### 6.1 Electrically open case

A visual representation of the effects of layer thickness, heterogeneous parameters, interfacial imperfection bonding parameters, and amplitudes of corrugation parameters on phase velocity is provided for the electrically open situation. In the structure under study, variation in wave number and phase velocity, as seen in Figs. 2-7, significantly impact how the Rayleigh wave propagates. Fig. 2 shows phase velocity versus wave number graphs for various inhomogeneity parameter values  $\alpha$  (0.03, 0.05, 0.07). This graph demonstrates that as wave number  $k$  rises, phase velocity monotonically falls. It grows once again as the wave number rises after reaching a lower level. The wave number falls as it rises for all values of  $\alpha$ . Fig. 3 shows the plots for wave number versus

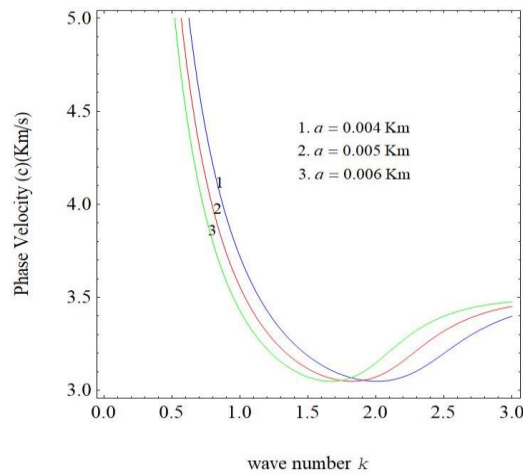


Fig. 4 Wave number versus phase velocity for various values of  $a$ : electrically open case

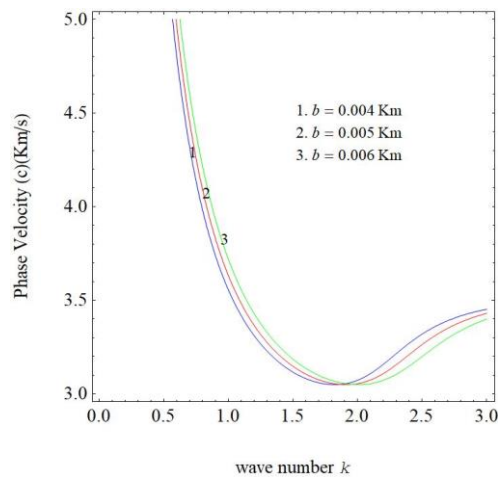


Fig. 5 Wave number versus phase velocity for various values of  $b$ : electrically open case

phase velocity for various values of layer thickness  $h$  (0.2 Km, 0.5 Km, 0.8 Km). It demonstrates that as wave number  $k$  rises, phase velocity falls. The wave number drops as  $h$  rises with all values of  $h$ . The graphs show that thickness change has a significant impact. After attaining lower level it again increasing with wave number. Figs. 4 and 5 reveal the effect of phase velocity due to variation in amplitudes of corrugation  $a$  ( $=0.008$  Km; 0.01 Km; 0.012 Km) and  $b$  ( $=0.008$  Km; 0.01 Km; 0.012 Km) respectively. Fig. 4 demonstrates phase velocity versus wave number for different values of amplitude of corrugation  $a$ , shows that the amplitude of corrugation  $a$  decreases with increasing the wave number whereas phase velocity decreases. After attaining the lower level the graphs become reversed and increasing as wave number increases. Fig. 5 demonstrates phase velocity versus wave number for different values of amplitude of corrugation  $b$ , shows that the amplitude of corrugation  $b$  increases with increasing the wave number whereas phase velocity decreases. After attaining lower level the nature of the graph become reversed as wave number increases phase velocity also increasing whereas  $b$  decreasing. Figs. 6 and 7 shows that the

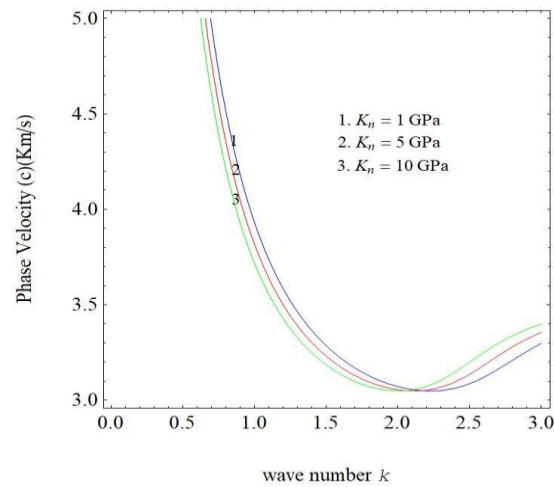


Fig. 6 Wave number versus phase velocity for various values of  $K_n$ : electrically open case

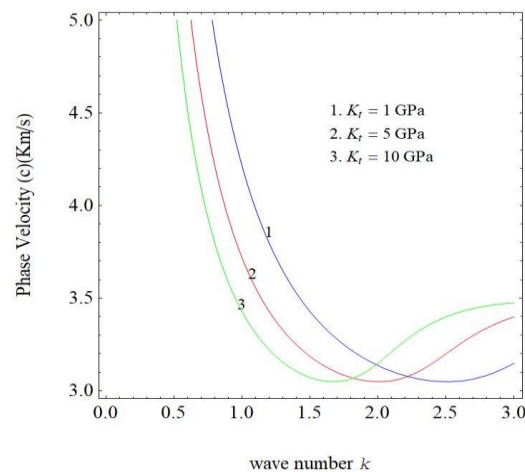


Fig. 7 Wave number versus phase velocity for various values of  $K_t$ : electrically open case

interfacial imperfection bonding parameters  $K_n$  and  $K_t$  are set to 1GPa,5GPa,10GPa respectively. Fig. 6, shows that interfacial imperfection bonding parameter  $K_n$  decreases with increasing the wave number whereas phase velocity falls. Once achieved  $k=2.0$ , graphs become reversed and increasing as wave number increases. Fig. 7, shows that interfacial imperfection bonding parameter  $K_n$  decreases with increasing the wave number whereas phase velocity decreases. The graphs show that variance has a massive effect. After attaining lower level it again increasing with wave number increases.

### 6.2 Electrically short case

For the electrically short case, the same material system is considered as used in the electrically open case. In the case of an electrically short structure, fluctuations between wave number and phase velocity, as seen in Figs. 8-13, significantly impact the propagation of the Rayleigh wave.

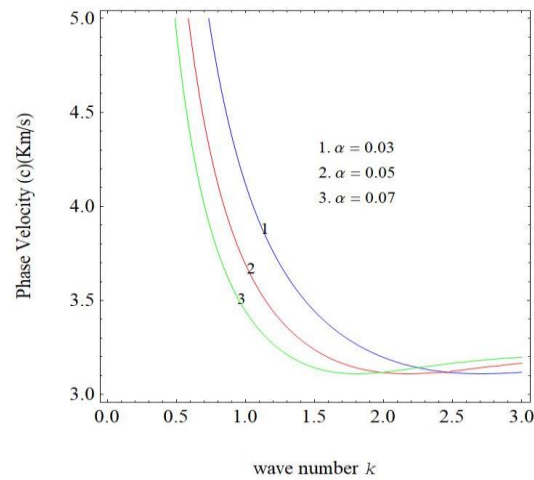


Fig. 8 Wave number versus phase velocity for various values of  $\alpha$ : electrically short case

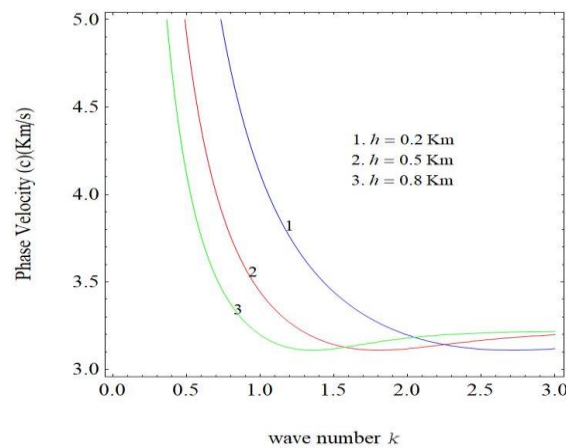
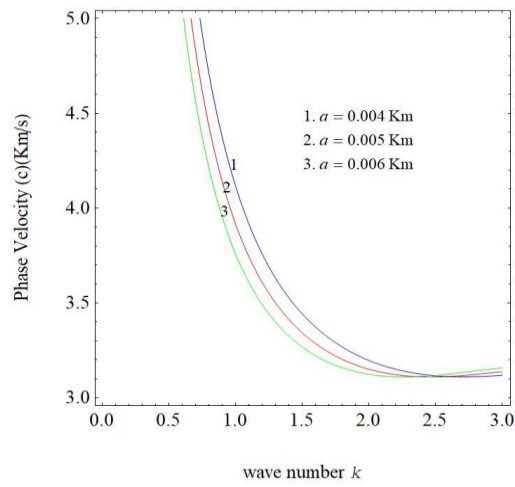
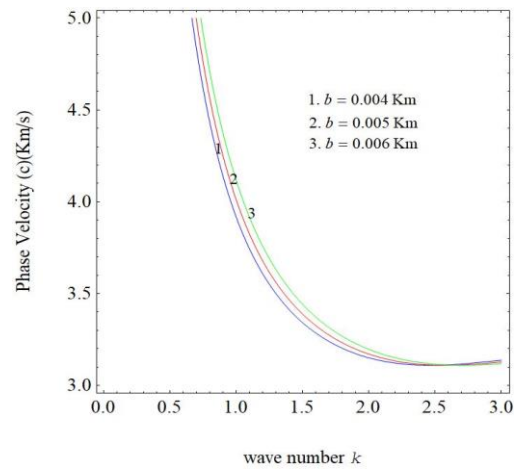
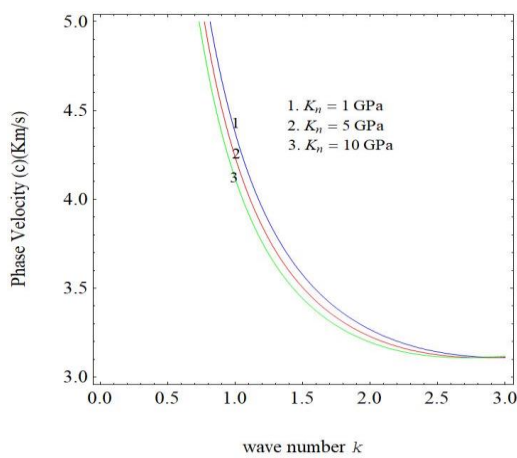


Fig. 9 Wave number versus phase velocity for various values of  $h$ : electrically short case

Fig. 8 shows the graphs for wave number versus phase velocity values for the inhomogeneity parameter  $\alpha$  (0.03,0.05,0.07). As can be observed in the open case, that phase velocity drops monotonically while the non - uniformity parameter  $\alpha$  falls as wave number  $k$  grows. Fig. 9 shows the plots for wave number versus phase velocity for different values of layer thickness  $h$  (0.2 Km, 0.5 Km, 0.8 Km). It demonstrates that when  $h$  decreases, wave number  $k$ 's phase velocity constantly decreases. The short example also exhibits a substantial influence of thickness variation, as in the open case. Figs. 10 and 11 reveal the effect of phase velocity due to variation in amplitudes of corrugation  $a$  ( $=0.008$  Km;  $0.01$  Km;  $0.012$  Km) and  $b$  ( $=0.008$  Km;  $0.01$  Km;  $0.012$  Km) respectively. Fig. 10 demonstrates phase velocity versus wave number for different values of amplitude of corrugation  $a$ , shows that the amplitude of corrugation decreases with increasing the wave number whereas phase velocity decreases and became merged. Fig. 5 demonstrates phase velocity versus wave number for different values of amplitude of corrugation  $b$ , showing that the amplitude of corrugation  $b$  increases with increasing the wave number whereas phase velocity decreases and became merged. Figs. 12 and 13 show that the interfacial imperfection bonding

Fig. 10 Wave number versus phase velocity for various values of  $a$ : electrically short caseFig. 11 Wave number versus phase velocity for various values of  $b$ : electrically short caseFig. 12 Wave number versus phase velocity for various values of  $K_n$ : electrically short case

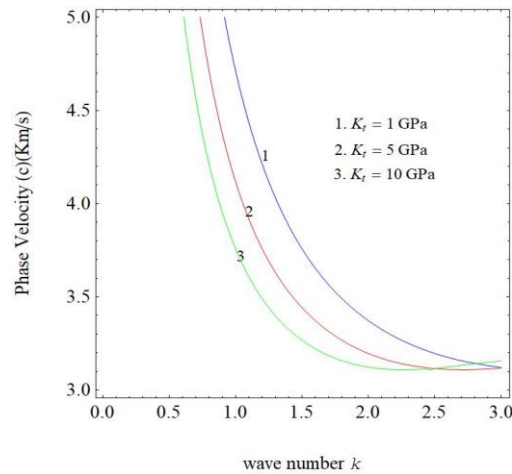


Fig. 13 Wave number versus phase velocity for various values of  $K_t$ : electrically short case

parameters  $K_n$  and  $K_t$  are set to 1 GPa, 5 GPa, 10 GPa respectively. Fig. 12 shows that the interfacial imperfection bonding parameter  $K_n$  decreases with increasing the wave number whereas phase velocity decreases. Fig. 13 shows the interfacial imperfection bonding parameter  $K_n$  decreases with increasing the wave number whereas phase velocity decreases. The graphs show that variance has a massive effect on  $K_t$ .

## 7. Conclusions

It is investigated how Rayleigh waves behave when propagating in an elastic substrate and an FGPM layer. The piezoelectric structure is comprised of a corrugated upper boundary and a loosely bonded corrugated interface. The determinant form establishes links between electrically open as well as short dispersion. For numerical modeling, FGPM layer and the elastic substrate were considered. The link between phase velocity and wavenumber is depicted in graphs using the numerical data. The conversation and aforementioned numerical data can be used to draw conclusions.

- In electrically open and electrically short cases, the depth, heterogeneity, interfacial defect bonding, and amplitudes of corrugation parameters all impact the Rayleigh wave's phase velocity.
- Generally, when the wavenumber rises, the phase velocity always falls.
- It was found that an FGPM medium's material gradient substantially impacts the Rayleigh wave's phase velocity. It is noted that phase velocity of the Rayleigh wave reduces with a reduction in the material gradient of an FGPM layer under both electrically open and electrically short conditions.
- The layer's thickness impacts electrically open and electrically short situations upon that phase velocity of the Rayleigh wave. For both electrically open & electrically short scenarios, the layer thickness reduces the Rayleigh wave's phase velocity value.
- The phase velocity of the Rayleigh wave is amplified by the imperfection parameter associated with the imperfect bonding of layer and half-space in both electrically short and

open situations.

- The phase velocity of Rayleigh wave is also affected by the amplitude of the corrugation parameter of upper boundary and it increases with the decreasing value of the corrugation parameter of upper boundary for both electrically open and electrically short cases.
- In both electrically open and short cases, it is seen that the effect of two corrugation amplitude parameters are in opposite in nature.
- It can be observed that seismic wave propagation is highly influenced by the thickness of layer, imperfect bonding of the layers and corrugation.
- The consequences of the study presented here find their application in the production and development of SAW devices.

## Acknowledgments

One of the authors express their sincere thanks to SRM Institute of Science and Technology, Kattankulathur, India, for providing the research fellowship and necessary research facility. Authors are also thankful to the reviewers for their valuable comments and suggestions to improve the quality of the paper.

## References

- Abubakar, I. (1962), "Reflection and refraction of plane SH waves at irregular interfaces. II", *J. Phys. Earth*, **10**(1), 15-20.
- Abubakar, I. (1962), "Scattering of plane elastic waves at rough surfaces. I", *Math. Proc. Cambridge Philos. Soc.*, **58**(1), 136-157.
- Asano, S. (1960), "Reflection and refraction of elastic waves at a corrugated boundary surface. Part I. The case of incidence of SH wave", *Bull. Earthq. Res. Inst., Univ. Tokyo*, **38**(2), 177-197.
- Asano, S. (1961), "Reflection and refraction of elastic waves at a corrugated boundary surface, II", *Bull. Earthq. Res. Inst., Univ. Tokyo*, **39**, 367-406.
- Asano, S. (1966), "Reflection and refraction of elastic waves at a corrugated interface", *Bull. Seismol. Soc. Am.*, **56**(1), 201-221. <https://doi.org/10.1785/BSSA0560010201>.
- Belyankova, T.I., Vorovich, E.I., Kalinchuk, V.V. and Tukodova, O.M. (2021), "Features of Rayleigh waves propagation in structures with FGPM coating made of various materials", *Physics and Mechanics of New Materials and Their Applications: Proceedings of the International Conference PHENMA 2020*, 245-259.
- Bubakar, I. (1962), "Reflection and Refraction of plane SH Waves at Irregular Interfaces I", *J. Phys. Earth*, **10**(1), 1-14.
- Cao, X., Jin, F., Jeon, I. and Lu, T.J. (2009), "Propagation of Love waves in a functionally graded piezoelectric material (FGPM) layered composite system", *Int. J. Solid. Struct.*, **46**(22-23), 4123-4132. <https://doi.org/10.1016/j.ijsolstr.2009.08.005>.
- Chaki, M.S. and Singh, A.K. (2020), "The impact of reinforcement and piezoelectricity on SH wave propagation in irregular imperfectly-bonded layered FGPM structures: An analytical approach", *Eur. J. Mech.-A/Solid.*, **80**, 103872. <https://doi.org/10.1016/j.euromechsol.2019.103872>.
- Du, J., Jin, X., Wang, J. and Xian, K. (2007), "Love wave propagation in functionally graded piezoelectric material layer", *Ultrasonic.*, **46**(1), 13-22. <https://doi.org/10.1016/j.ultras.2006.09.004>.
- Dunkin, J.W. and Eringen, A.C. (1962), "The reflection of elastic waves from a free or fixed, wavy boundary of a half-space", *Proceedings of the 4th U.S. National Congress on Applied Mechanics*, Berkeley, 143-160.

- Guo, F.L. and Sun, R. (2008), "Propagation of Bleustein–Gulyaev wave in 6 mm piezoelectric materials loaded with viscous liquid", *Int. J. Solid. Struct.*, **45**(13), 3699-3710. <https://doi.org/10.1016/j.ijsolstr.2007.09.018>.
- Gupta, S. (1987), "Reflection and transmission of SH-waves in laterally and vertically heterogeneous media at an irregular boundary", *Geophys. Transac.*, **33**(2), 89-111.
- Hemalatha, K., Kumar, S. and Prakash, D. (2023), "Dispersion of Rayleigh wave in a functionally graded piezoelectric layer over elastic substrate", *Forc. Mech.*, **10**, 100171. <https://doi.org/10.1016/j.finmec.2023.100171>.
- Hua, L.I.U., Yang, J.L. and Liu, K.X. (2007), "Love waves in layered graded composite structures with imperfectly bonded interface", *Chin. J. Aeronaut.*, **20**(3), 210-214. [https://doi.org/10.1016/S1000-9361\(07\)60034-X](https://doi.org/10.1016/S1000-9361(07)60034-X).
- Jakoby, B. and Vellekoop, M.J. (1997), "Properties of Love waves: Applications in sensors", *Smart Mater. Struct.*, **6**(6), 668.
- Jin, F., Qian, Z., Wang, Z. and Kishimoto, K. (2005), "Propagation behavior of Love waves in a piezoelectric layered structure with inhomogeneous initial stress", *Smart Mater. Struct.*, **14**(4), 515. <https://doi.org/10.1088/0964-1726/14/4/009>.
- Jones, J.P. and Whittier, J.S. (1967), "Waves at a flexibly bonded interface", *Appl. Mech.*, **34**(4), 905-909. <https://doi.org/10.1115/1.3607854>.
- Kaur, J., Tomar, S.K. and Kaushik, V.P. (2005), "Reflection and refraction of SH-waves at a corrugated interface between two laterally and vertically heterogeneous viscoelastic solid half-spaces", *Int. J. Solid. Struct.*, **42**(13), 3621-43. <https://doi.org/10.1016/j.ijsolstr.2004.11.014>.
- Kumar, R., Tomar, S.K. and Chopra, A. (2003), "Reflection/refraction of SH-waves at a corrugated interface between two different anisotropic and vertically heterogeneous elastic solid half-spaces", *ANZIAM J.*, **44**(3), 447-460. <https://doi.org/10.1017/S1446181100008130>.
- Kundu, S., Manna, S. and Gupta, S. (2014), "Love wave dispersion in pre-stressed homogeneous medium over a porous half-space with irregular boundary surfaces", *Int. J. Solid. Struct.*, **51**(21-22), 3689-3697. <https://doi.org/10.1016/j.ijsolstr.2014.07.002>.
- Lavrentyev, A.I. and Rokhlin, S.I. (1998), "Ultrasonic spectroscopy of imperfect contact interfaces between a layer and two solids", *J. Acoust. Soc. Am.*, **103**(2), 657-664. <https://doi.org/10.1121/1.423235>.
- Li, K., Jing, S., Yu, J. and Zhang, B. (2021), "Complex Rayleigh waves in nonhomogeneous magneto-electro-elastic half-spaces", *Mater.*, **14**(4), 1011. <https://doi.org/10.3390/ma14041011>.
- Li, X.Y., Wang, Z.K. and Huang, S.H. (2004), "Love waves in functionally graded piezoelectric materials", *Int. J. Solid. Struct.*, **41**(26), 7309-7328. <https://doi.org/10.1016/j.ijsolstr.2004.05.064>.
- Liang, Y., Li, Y., Liu, Y., Han, Q. and Liu, D. (2019), "Investigation of wave propagation in piezoelectric helical waveguides with the spectral finite element method", *Compos. Part B: Eng.*, **160**, 205- 216. <https://doi.org/10.1016/j.compositesb.2018.09.083>.
- Liu, C., Yu, J., Zhang, B., Zhang, X. and Elmaimouni, L. (2021), "Analysis of Lamb wave propagation in a functionally graded piezoelectric small-scale plate based on the modified couple stress theory", *Compos. Struct.*, **265**, 113733. <https://doi.org/10.1016/j.compstruct.2021.113733>.
- Liu, G.R., Han, X. and Lam, K.Y. (1999), "Stress waves in functionally gradient materials and its use for material characterization", *Compos. Part B: Eng.*, **30**(4), 383-394. [https://doi.org/10.1016/S1359-8368\(99\)00010-4](https://doi.org/10.1016/S1359-8368(99)00010-4).
- Liu, Y., Lin, S., Li, Y., Li, C. and Liang, Y. (2019), "Numerical investigation of Rayleigh waves in layered composite piezoelectric structures using the SIGA-PML approach", *Compos. Part B: Eng.*, **158**, 230-238. <https://doi.org/10.1016/j.compositesb.2018.09.037>.
- Murty, G. (1975), "A theoretical model for the attenuation and dispersion of Stoneley waves at the loosely bonded interface of elastic half spaces", *Phys. Earth Planet. Interior.*, **11**(1), 65-79. [https://doi.org/10.1016/0031-9201\(75\)90076-X](https://doi.org/10.1016/0031-9201(75)90076-X).
- Pal, P.C., Kumar, S. and Bose, S. (2015), "Propagation of Rayleigh waves in anisotropic layer overlying a semi-infinite sandy medium", *Ain Shams Eng. J.*, **6**(2), 621-627. <https://doi.org/10.1016/j.asej.2014.11.003>.

- Qian, Z., Jin, F., Wang, Z. and Kishimoto, K. (2004), "Love waves propagation in a piezoelectric layered structure with initial stresses", *Acta Mechanica*, **171**, 41-57. <https://doi.org/10.1007/s00707-004-0128-8>.
- Ray, A. and Singh, A.K. (2021), "Impact of imperfect corrugated interface in piezoelectric-piezomagnetic composites on reflection and refraction of plane waves", *J. Acoust. Soc. Am.*, **150**(1), 573-591. <https://doi.org/10.1121/10.0005544>.
- Saha, S., Singh, A.K. and Chattopadhyay, A. (2021), "Impact of curved boundary on the propagation characteristics of Rayleigh-type wave and SH-wave in a prestressed monoclinic media", *Mech. Adv. Mater. Struct.*, **28**(12), 1274-1287. <https://doi.org/10.1080/15376494.2019.1660930>.
- Singh, A.K., Kumar, S. and Chattopadhyay, A. (2014), "Effect of irregularity and heterogeneity on the stresses produced due to a normal moving load on a rough monoclinic half-space", *Meccanica*, **49**, 2861-2878. <https://doi.org/10.1007/s11012-014-0033-8>.
- Singh, S.S. (2011), "Love wave at a layer medium bounded by irregular boundary surfaces", *J. Vib. Control*, **17**(5), 789-795. <https://doi.org/10.1177/10775463093513>.
- Singh, S.S. (2011), "Response of shear wave from a corrugated interface between elastic solid/viscoelastic half-spaces", *Int. J. Numer. Anal. Meth. Geomech.*, **35**(5), 529- 543. <https://doi.org/10.1002/nag.901>.
- Singh, S.S. and Tomar, S.K. (2008), "qP-wave at a corrugated interface between two dissimilar pre-stressed elastic half-spaces", *J. Sound Vib.*, **317**(3-5), 687-708. <https://doi.org/10.1016/j.jsv.2008.03.036>.
- Singhal, A., Sahu, S.A. and Chaudhary, S. (2018), "Approximation of surface wave frequency in piezocomposite structure", *Compos. Part B: Eng.*, **144**, 19-28. <https://doi.org/10.1016/j.compositesb.2018.01.017>.
- Slavin, L.M. and Wolf, B. (1970), "Scattering of Love waves in a surface layer with an irregular boundary for the case of a rigid underlying half-space", *Bull. Seismol. Soc. Am.*, **60**(3), 859-877. <https://doi.org/10.1785/BSSA0600030859>.
- Sumner, J.H. and Deresiewicz, H. (1972), "Waves in an elastic plate with an irregular boundary", *Pure Appl. Geophys.*, **96**, 106-126. <https://doi.org/10.1007/BF00875633>.
- Tomar, S., Kumar, R. and Chopra, A. (2002), "Reflection/refraction of SH waves at a corrugated interface between transversely isotropic and visco-elastic solid half-spaces", *Acta Geophysica Polonica*, **50**(2), 231-249.
- Tomar, S.K. and Kaur, J. (2003), "Reflection and transmission of SH-waves at a corrugated interface between two laterally and vertically heterogeneous anisotropic elastic solid half-spaces", *Earth Planet. Space*, **55**(9), 531-547.
- Tomar, S.K. and Kaur, J. (2007), "SH-waves at a corrugated interface between a dry sandy half-space and an anisotropic elastic half-space", *Acta Mechanica*, **190**(1-4), 1-28. <https://doi.org/10.1007/s00707-006-0423-7>.
- Tomar, S.K. and Saini, S.L. (1997), "Reflection and refraction of SH-waves at a corrugated interface between two-dimensional transversely isotropic half-spaces", *J. Phys. Earth*, **45**(5), 347-62.
- Tomar, S.K. and Sarat Singh, S. (2006), "Plane SH-waves at a corrugated interface between two dissimilar perfectly conducting self-reinforced elastic half-spaces", *Int. J. Numer. Anal. Meth. Geomech.*, **30**(6), 455-487. <https://doi.org/10.1002/nag.485>.
- Wu, T.T. and Wu, T.Y. (2000), "Surface waves in coated anisotropic medium loaded with viscous liquid", *J. Appl. Mech.*, **67**(2), 262-266. <https://doi.org/10.1115/1.1304840>.
- Zhang, R. and Shinozuka, M. (1996), "Effects of irregular boundaries in a layered half-space on seismic waves", *J. Sound Vib.*, **195**(1), 1-16. <https://doi.org/10.1006/jsvi.1996.0400>.

**Appendix A**

$$\begin{aligned}
a_{11} &= C_{44}^{(10)} s^2 - \frac{\alpha}{k} C_{44}^{(10)} s + \rho_1 c^2 - C_{11}^{(10)}, a_{12} = (i) \left\{ - \left( C_{13}^{(10)} + C_{44}^{(10)} \right) s + \frac{\alpha}{k} C_{44}^{(10)} \right\}, \\
a_{13} &= (i) \left\{ - \left( e_{31}^{(10)} + e_{15}^{(10)} \right) s + \frac{\alpha}{k} e_{15}^{(10)} \right\}, a_{21} = (i) \left\{ - \left( C_{44}^{(10)} + C_{13}^{(10)} \right) s + \frac{\alpha}{k} C_{13}^{(10)} \right\}, \\
a_{22} &= C_{33}^{(10)} s^2 - \frac{\alpha}{k} C_{33}^{(10)} s + \rho_1 c^2 - C_{44}^{(10)}, a_{23} = e_{33}^{(10)} s^2 - \frac{\alpha}{k} e_{33}^{(10)} s - e_{15}^{(10)}, \\
a_{31} &= -(i) \left( e_{15}^{(10)} + e_{31}^{(10)} \right) s + \frac{\alpha}{k} e_{31}^{(10)}, a_{32} = - \left( e_{33}^{(10)} s^2 - \frac{\alpha}{k} e_{33}^{(10)} s + e_{15}^{(10)} \right), \\
a_{33} &= \kappa_{33}^{(10)} s^2 - \frac{\alpha}{k} \kappa_{33}^{(10)} s - \kappa_{11}^{(10)}.
\end{aligned}$$

**Appendix B**

$$\begin{aligned}
a_0 &= C_{44}^{(10)} \left( e_{33}^{(10)} \right)^2 + C_{33}^{(10)} C_{44}^{(10)} \kappa_{33}^{(10)}, a_1 = \frac{\alpha C_{44}^{(10)} \left( e_{33}^{(10)} \right)^2}{k} - \frac{3\alpha C_{33}^{(10)} C_{44}^{(10)} \kappa_{33}^{(10)}}{k}, \\
a_2 &= C_{33}^{(10)} \left( e_{15}^{(10)} \right)^2 + 2C_{33}^{(10)} e_{15}^{(10)} e_{31}^{(10)} + C_{33}^{(10)} \left( e_{15}^{(10)} \right)^2 - 2C_{44}^{(10)} e_{15}^{(10)} e_{33}^{(10)} - C_{11}^{(10)} \left( e_{33}^{(10)} \right)^2 \\
&\quad - \frac{\alpha^2 C_{44}^{(10)} \left( e_{33}^{(10)} \right)^2}{k^2} - C_{33}^{(10)} C_{44}^{(10)} \kappa_{11}^{(10)} + C_{11}^{(10)} C_{33}^{(10)} \kappa_{33}^{(10)} + 2C_{13}^{(10)} C_{44}^{(10)} \kappa_{33}^{(10)} \\
&\quad + \frac{3\alpha^2 C_{33}^{(10)} C_{44}^{(10)} \kappa_{33}^{(10)}}{k^2} + c^2 \left( e_{33}^{(10)} \right)^2 \rho_{10} + c^2 C_{33}^{(10)} \kappa_{33}^{(10)} \rho_{10} + c^2 C_{44}^{(10)} \kappa_{33}^{(10)} \rho_{10}, \\
a_3 &= \frac{\alpha^3 C_{44}^{(10)} \left( e_{33}^{(10)} \right)^2}{k^3} - \frac{2\alpha C_{33}^{(10)} \left( e_{15}^{(10)} \right)^2}{k} - \frac{2\alpha C_{33}^{(10)} e_{15}^{(10)} e_{31}^{(10)}}{k} + \frac{4\alpha C_{44}^{(10)} e_{15}^{(10)} e_{33}^{(10)}}{k} \\
&\quad + \frac{2\alpha C_{44}^{(10)} e_{31}^{(10)} e_{33}^{(10)}}{k} + \frac{2\alpha C_{33}^{(10)} C_{44}^{(10)} \kappa_{11}^{(10)}}{k} - \frac{\alpha^3 C_{33}^{(10)} C_{44}^{(10)} \kappa_{33}^{(10)}}{k^3} - \frac{2\alpha \left( C_{13}^{(10)} \right)^2 \kappa_{11}^{(10)}}{k} \\
&\quad + \frac{2\alpha C_{11}^{(10)} C_{33}^{(10)} \kappa_{33}^{(10)}}{k} - \frac{4\alpha C_{13}^{(10)} C_{44}^{(10)} \kappa_{33}^{(10)}}{k} - \frac{2\alpha c^2 C_{33}^{(10)} \kappa_{33}^{(10)} \rho_{10}}{k} - \frac{2\alpha c^2 C_{44}^{(10)} \kappa_{33}^{(10)} \rho_{10}}{k}, \\
a_4 &= -2C_{33}^{(10)} e_{15}^{(10)} e_{31}^{(10)} - C_{44}^{(10)} \left( e_{31}^{(10)} \right)^2 + 2C_{11}^{(10)} e_{15}^{(10)} e_{33}^{(10)} + \frac{\alpha^2 C_{33}^{(10)} \left( e_{15}^{(10)} \right)^2}{k^2} \\
&\quad - \frac{\alpha^2 C_{33}^{(10)} e_{15}^{(10)} e_{31}^{(10)}}{k^2} - \frac{\alpha^2 C_{33}^{(10)} \left( e_{31}^{(10)} \right)^2}{k^2} - \frac{\alpha^2 C_{13}^{(10)} e_{15}^{(10)} e_{31}^{(10)}}{k^2} - \frac{2\alpha^2 C_{44}^{(10)} e_{15}^{(10)} e_{33}^{(10)}}{k^2} \\
&\quad + \frac{\alpha^2 C_{44}^{(10)} e_{31}^{(10)} e_{33}^{(10)}}{k^2} + \frac{\alpha^2 C_{11}^{(10)} \left( e_{33}^{(10)} \right)^2}{k^2} - \left( C_{13}^{(10)} \right)^2 \kappa_{11}^{(10)} + C_{11}^{(10)} C_{33}^{(10)} \kappa_{11}^{(10)} \\
&\quad - 2C_{13}^{(10)} C_{44}^{(10)} \kappa_{11}^{(10)} - \frac{\alpha^2 C_{33}^{(10)} C_{44}^{(10)} \kappa_{11}^{(10)}}{k^2} + C_{11}^{(10)} C_{44}^{(10)} \kappa_{33}^{(10)} + \frac{\alpha^2 \left( C_{13}^{(10)} \right)^2 \kappa_{33}^{(10)}}{k^2} \\
&\quad - \frac{\alpha^2 C_{11}^{(10)} C_{33}^{(10)} \kappa_{33}^{(10)}}{k^2} + \frac{3\alpha^2 C_{13}^{(10)} C_{44}^{(10)} \kappa_{33}^{(10)}}{k^2} + c^2 \left( e_{15}^{(10)} \right)^2 \rho_{10} + 2c^2 e_{15}^{(10)} e_{31}^{(10)} \rho_{10}
\end{aligned}$$

$$\begin{aligned}
& +c^2 \left( e_{31}^{(10)} \right)^2 \rho_{10} - 2c^2 e_{15}^{(10)} e_{33}^{(10)} \rho_{10} - \frac{\alpha^2 c^2 \left( e_{33}^{(10)} \right)^2 \rho_{10}}{k^2} - c^2 C_{33}^{(10)} \kappa_{11}^{(10)} \rho_{10} - c^2 C_{44}^{(10)} \kappa_{11}^{(10)} \rho_{10} \\
& - c^2 C_{11}^{(10)} \kappa_{33}^{(10)} \rho_{10} - c^2 C_{44}^{(10)} \kappa_{33}^{(10)} \rho_{10} + \frac{\alpha^2 c^2 C_{33}^{(10)} \kappa_{33}^{(10)} \rho_{10}}{k^2} + \frac{\alpha^2 c^2 C_{44}^{(10)} \kappa_{33}^{(10)} \rho_{10}}{k^2} + c^4 \kappa_{33}^{(10)} \rho_{10}^2, \\
a_5 = & \frac{\alpha^3 C_{33}^{(10)} e_{15}^{(10)} e_{31}^{(10)}}{k^3} + \frac{\alpha^3 C_{13}^{(10)} e_{15}^{(10)} e_{33}^{(10)}}{k^3} - \frac{\alpha^3 C_{44}^{(10)} e_{31}^{(10)} e_{31}^{(10)}}{k^3} + \frac{2\alpha C_{13}^{(10)} e_{15}^{(10)} e_{31}^{(10)}}{k} \\
& - \frac{2\alpha C_{13}^{(10)} \left( e_{15}^{(10)} \right)^2}{k} - \frac{2\alpha C_{44}^{(10)} \left( e_{31}^{(10)} \right)^2}{k} + \frac{\alpha \left( C_{13}^{(10)} \right)^2 \kappa_{11}^{(10)}}{k} - \frac{\alpha C_{11}^{(10)} C_{33}^{(10)} \kappa_{11}^{(10)}}{k} \\
& + \frac{\alpha C_{13}^{(10)} C_{44}^{(10)} \kappa_{11}^{(10)}}{k} - \frac{\alpha^3 C_{13}^{(10)} C_{44}^{(10)} \kappa_{33}^{(10)}}{k^3} - \frac{\alpha C_{11}^{(10)} C_{44}^{(10)} \kappa_{33}^{(10)}}{k} - \frac{\alpha c^2 \left( e_{15}^{(10)} \right)^2 \rho_{10}}{k} \\
& + \frac{\alpha c^2 \left( e_{31}^{(10)} \right)^2 \rho_{10}}{k} + \frac{\alpha c^2 C_{33}^{(10)} \kappa_{11}^{(10)} \rho_{10}}{k} + \frac{\alpha c^2 C_{44}^{(10)} \kappa_{11}^{(10)} \rho_{10}}{k} + \frac{\alpha c^2 C_{11}^{(10)} \kappa_{33}^{(10)} \rho_{10}}{k} \\
& + \frac{\alpha c^2 C_{44}^{(10)} \kappa_{33}^{(10)} \rho_{10}}{k} + \frac{\alpha c^4 \kappa_{33}^{(10)} \rho_{10}^2}{k}, \\
a_6 = & -C_{11}^{(10)} \left( e_{31}^{(10)} \right)^2 - \frac{\alpha^2 C_{13}^{(10)} \left( e_{15}^{(10)} \right)^2}{k^2} - C_{11}^{(10)} C_{44}^{(10)} \kappa_{11}^{(10)} - \frac{\alpha^2 C_{13}^{(10)} C_{44}^{(10)} \kappa_{11}^{(10)}}{k^2} \\
& + c^2 \left( e_{15}^{(10)} \right)^2 \rho_{10} - \frac{\alpha^2 c^2 e_{15}^{(10)} e_{31}^{(10)} \rho_{10}}{k^2} + c^2 C_{11}^{(10)} \kappa_{11}^{(10)} \rho_{10} + c^2 C_{44}^{(10)} \kappa_{11}^{(10)} \rho_{10} - c^4 \kappa_{11}^{(10)} \rho_{10}^2.
\end{aligned}$$

### Appendix C

$$\begin{aligned}
a_{11j} &= C_{44}^{(10)} s_j^2 - \frac{\alpha}{k} C_{44}^{(10)} s_j + \rho_1 c^2 - C_{11}^{(10)}, a_{12j} = (i) \left\{ - \left( C_{13}^{(10)} + C_{44}^{(10)} \right) s_j + \frac{\alpha}{k} C_{44}^{(10)} \right\}, \\
a_{13j} &= (i) \left\{ - \left( e_{31}^{(10)} + e_{15}^{(10)} \right) s_j + \frac{\alpha}{k} e_{15}^{(10)} \right\}, a_{21j} = (i) \left\{ - \left( C_{44}^{(10)} + C_{13}^{(10)} \right) s_j + \frac{\alpha}{k} C_{13}^{(10)} \right\}, \\
a_{22j} &= C_{33}^{(10)} s_j^2 - \frac{\alpha}{k} C_{33}^{(10)} s_j + \rho_1 c^2 - C_{44}^{(10)}, a_{23j} = e_{33}^{(10)} s_j^2 - \frac{\alpha}{k} e_{33}^{(10)} s_j - e_{15}^{(10)}, \\
a_{31j} &= -(i) \left( e_{15}^{(10)} + e_{31}^{(10)} \right) s_j + \frac{\alpha}{k} e_{31}^{(10)}, a_{32j} = - \left( e_{33}^{(10)} s_j^2 - \frac{\alpha}{k} e_{33}^{(10)} s_j + e_{15}^{(10)} \right), \\
a_{33j} &= \kappa_{33}^{(10)} s_j^2 - \frac{\alpha}{k} \kappa_{33}^{(10)} s_j - \kappa_{11}^{(10)}, (j = 1, \dots, 6)
\end{aligned}$$

### Appendix D

$$\begin{aligned}
b_{11} &= C_{44}^{(20)} q^2 + \rho_2 c^2 - C_{11}^{(20)}, b_{12} = (-iq) \left( C_{13}^{(20)} + C_{44}^{(20)} \right), \\
b_{21} &= (-iq) \left( C_{44}^{(20)} + C_{13}^{(20)} \right), b_{22} = C_{33}^{(20)} q^2 + \rho_2 c^2 - C_{44}^{(20)}.
\end{aligned}$$

**Appendix E**

$$b_0 = C_{44}^{(20)} C_{33}^{(20)}, b_1 = C_{44}^{(20)} \rho_2 c^2 + C_{33}^{(20)} \rho_2 c^2 - C_{11}^{(20)} C_{33}^{(20)} + 2C_{44}^{(20)} C_{33}^{(20)} + \left(C_{33}^{(20)}\right)^2,$$

$$b_2 = (\rho_2)^2 C_{44}^{(20)} - \left(C_{44}^{(20)} + C_{11}^{(20)}\right) \rho_2 c^2 - C_{44}^{(20)} C_{11}^{(20)}.$$

**Appendix F**

$$b_{11j} = C_{44}^{(20)} q_j^2 + \rho_2 c^2 - C_{11}^{(20)}, b_{12j} = (-iq_j) \left(C_{13}^{(20)} + C_{44}^{(20)}\right), (j = 1, 2)$$

**Appendix G**

$$m_{11} = m_{18} = m_{19} = m_{110} = 0,$$

$$m_{12} = \left\{ iC_{13}^{(10)} - \delta_{11} s_1 C_{33}^{(10)} - \gamma_{11} s_1 e_{33}^{(10)} \right. \\ \left. - g_2' \left[ C_{44}^{(10)} (i\delta_{11} - s_1) + i e_{15}^{(10)} \gamma_{11} \right] \right\} e^{-ks_1[-h+g_2]},$$

$$m_{13} = \left\{ iC_{13}^{(10)} - \delta_{12} s_2 C_{33}^{(10)} - \gamma_{12} s_2 e_{33}^{(10)} \right. \\ \left. - g_2' \left[ C_{44}^{(10)} (i\delta_{12} - s_2) + i e_{15}^{(10)} \gamma_{12} \right] \right\} e^{-ks_2[-h+g_2]},$$

$$m_{14} = \left\{ iC_{13}^{(10)} - \delta_{12} s_3 C_{33}^{(10)} - \gamma_{13} s_3 e_{33}^{(10)} \right. \\ \left. - g_2' \left[ C_{44}^{(10)} (i\delta_{13} - s_3) + i e_{15}^{(10)} \gamma_{13} \right] \right\} e^{-ks_3[-h+g_2]},$$

$$m_{15} = \left\{ iC_{13}^{(10)} - \delta_{14} s_4 C_{33}^{(10)} - \gamma_{14} s_4 e_{33}^{(10)} \right. \\ \left. - g_2' \left[ C_{44}^{(10)} (i\delta_{14} - s_4) + i e_{15}^{(10)} \gamma_{14} \right] \right\} e^{-ks_4[-h+g_2]},$$

$$m_{16} = \left\{ iC_{13}^{(10)} - \delta_{15} s_5 C_{33}^{(10)} - \gamma_{15} s_5 e_{33}^{(10)} \right. \\ \left. - g_2' \left[ C_{44}^{(10)} (i\delta_{15} - s_5) + i e_{15}^{(10)} \gamma_{15} \right] \right\} e^{-ks_5[-h+g_2]},$$

$$m_{17} = \left\{ iC_{13}^{(10)} - \delta_{16} s_6 C_{33}^{(10)} - \gamma_{16} s_6 e_{33}^{(10)} \right. \\ \left. - g_2' \left[ C_{44}^{(10)} (i\delta_{16} - s_6) + i e_{15}^{(10)} \gamma_{16} \right] \right\} e^{-ks_6[-h+g_2]},$$

$$m_{21} = m_{28} = m_{29} = m_{210} = 0,$$

$$m_{22} = \left\{ C_{44}^{(10)} (i\delta_{11} - s_1) + i e_{15}^{(10)} \gamma_{11} \right. \\ \left. - g_2' \left[ iC_{11}^{(10)} - \delta_{11} s_1 C_{13}^{(10)} - \gamma_{11} s_1 e_{33}^{(10)} \right] \right\} e^{-ks_1[-h+g_2]},$$

$$m_{23} = \left\{ C_{44}^{(10)} (i\delta_{12} - s_2) + i e_{15}^{(10)} \gamma_{12} \right. \\ \left. - g_2' \left[ iC_{11}^{(10)} - \delta_{12} s_2 C_{13}^{(10)} - \gamma_{12} s_2 e_{33}^{(10)} \right] \right\} e^{-ks_2[-h+g_2]},$$

$$m_{24} = \left\{ C_{44}^{(10)} (i\delta_{13} - s_3) + i e_{15}^{(10)} \gamma_{13} \right. \\ \left. - g_2' \left[ iC_{11}^{(10)} - \delta_{13} s_3 C_{13}^{(10)} - \gamma_{13} s_3 e_{33}^{(10)} \right] \right\} e^{-ks_3[-h+g_2]},$$

$$\begin{aligned}
m_{26} &= \left\{ C_{44}^{(10)}(i\delta_{15} - s_5) + ie_{15}^{(10)}\gamma_{15} \right. \\
&\quad \left. - g_2' \left[ iC_{11}^{(10)} - \delta_{15}s_5C_{13}^{(10)} - \gamma_{15}s_5e_{33}^{(10)} \right] \right\} e^{-ks_5[-h+g_2]}, \\
m_{27} &= \left\{ C_{44}^{(10)}(i\delta_{16} - s_6) + ie_{15}^{(10)}\gamma_{16} \right. \\
&\quad \left. - g_2' \left[ iC_{11}^{(10)} - \delta_{16}s_6C_{13}^{(10)} - \gamma_{16}s_6e_{33}^{(10)} \right] \right\} e^{-ks_6[-h+g_2]}, \\
m_{31} &= e^{k[-h+g_2]}, m_{38} = m_{39} = m_{310} = 0, \\
m_{32} &= -\gamma_{11}e^{ks_1[-h+g_2]}, m_{33} = -\gamma_{12}e^{ks_2[-h+g_2]}, \\
m_{34} &= -\gamma_{13}e^{ks_3[-h+g_2]}, m_{35} = -\gamma_{14}e^{ks_4[-h+g_2]}, \\
m_{36} &= -\gamma_{15}e^{ks_5[-h+g_2]}, m_{37} = -\gamma_{16}e^{ks_6[-h+g_2]}, \\
m_{41} &= \varepsilon_0 e^{k[-h+g_2]}, m_{48} = m_{49} = m_{410} = 0, \\
m_{42} &= \left\{ ie_{31}^{(10)} - e_{33}^{(10)}\delta_{11}s_1 + \kappa_{33}^{(10)}\gamma_{11}s_1 \right\} e^{a[-h+g_2]}e^{ks_1[-h+g_2]}, \\
m_{43} &= \left\{ ie_{31}^{(10)} - e_{33}^{(10)}\delta_{12}s_2 + \kappa_{33}^{(10)}\gamma_{12}s_2 \right\} e^{a[-h+g_2]}e^{ks_2[-h+g_2]}, \\
m_{44} &= \left\{ ie_{31}^{(10)} - e_{33}^{(10)}\delta_{13}s_3 + \kappa_{33}^{(10)}\gamma_{13}s_3 \right\} e^{a[-h+g_2]}e^{ks_3[-h+g_2]}, \\
m_{45} &= \left\{ ie_{31}^{(10)} - e_{33}^{(10)}\delta_{14}s_4 + \kappa_{33}^{(10)}\gamma_{14}s_4 \right\} e^{a[-h+g_2]}e^{ks_4[-h+g_2]}, \\
m_{46} &= \left\{ ie_{31}^{(10)} - e_{33}^{(10)}\delta_{15}s_5 + \kappa_{33}^{(10)}\gamma_{15}s_5 \right\} e^{a[-h+g_2]}e^{ks_5[-h+g_2]}, \\
m_{47} &= \left\{ ie_{31}^{(10)} - e_{33}^{(10)}\delta_{16}s_6 + \kappa_{33}^{(10)}\gamma_{16}s_6 \right\} e^{a[-h+g_2]}e^{ks_6[-h+g_2]}, \\
m_{61} &= m_{68} = 0, \\
m_{62} &= K_t e^{-ks_1g_1}, m_{63} = K_t e^{-ks_2g_1}, m_{64} = K_t e^{-ks_3g_1}, \\
m_{65} &= K_t e^{-ks_4g_1}, m_{66} = K_t e^{-ks_5g_1}, m_{67} = K_t e^{-ks_6g_1}, \\
m_{69} &= -\left\{ C_{44}^{(20)}(ik\delta_{21} - kq_1) - g_1' \left[ ikC_{11}^{(20)} - kC_{13}^{(20)}\delta_{21}q_1 \right] + K_t \right\} e^{-kq_1g_1}, \\
m_{610} &= -\left\{ C_{44}^{(20)}(ik\delta_{22} - kq_2) - g_1' \left[ ikC_{11}^{(20)} - kC_{13}^{(20)}\delta_{22}q_2 \right] + K_t \right\} e^{-kq_2g_1}, \\
m_{71} &= m_{78} = 0, \\
m_{72} &= \left\{ iC_{13}^{(10)} - \delta_{11}s_1C_{33}^{(10)} - \gamma_{11}s_1e_{33}^{(10)} \right. \\
&\quad \left. - g_1' \left[ C_{44}^{(10)}(i\delta_{11} - s_1) + ie_{15}^{(10)}\gamma_{11} \right] \right\} e^{ag_1}e^{-ks_1g_1}, \\
m_{73} &= \left\{ iC_{13}^{(10)} - \delta_{12}s_2C_{33}^{(10)} - \gamma_{12}s_2e_{33}^{(10)} \right. \\
&\quad \left. - g_1' \left[ C_{44}^{(10)}(i\delta_{12} - s_2) + ie_{15}^{(10)}\gamma_{12} \right] \right\} e^{ag_1}e^{-ks_2g_1}, \\
m_{74} &= \left\{ iC_{13}^{(10)} - \delta_{13}s_3C_{33}^{(10)} - \gamma_{13}s_3e_{33}^{(10)} \right. \\
&\quad \left. - g_1' \left[ C_{44}^{(10)}(i\delta_{13} - s_3) + ie_{15}^{(10)}\gamma_{13} \right] \right\} e^{ag_1}e^{-ks_3g_1}, \\
m_{75} &= \left\{ iC_{13}^{(10)} - \delta_{14}s_4C_{33}^{(10)} - \gamma_{14}s_4e_{33}^{(10)} \right. \\
&\quad \left. - g_1' \left[ C_{44}^{(10)}(i\delta_{14} - s_4) + ie_{15}^{(10)}\gamma_{14} \right] \right\} e^{ag_1}e^{-ks_4g_1}, \\
m_{76} &= \left\{ iC_{13}^{(10)} - \delta_{15}s_5C_{33}^{(10)} - \gamma_{15}s_5e_{33}^{(10)} \right. \\
&\quad \left. - g_1' \left[ C_{44}^{(10)}(i\delta_{15} - s_5) + ie_{15}^{(10)}\gamma_{15} \right] \right\} e^{ag_1}e^{-ks_5g_1}, \\
m_{77} &= \left\{ iC_{13}^{(10)} - \delta_{16}s_6C_{33}^{(10)} - \gamma_{16}s_6e_{33}^{(10)} \right.
\end{aligned}$$

$$\begin{aligned}
& -g_1' \left[ C_{44}^{(10)} (i\delta_{16} - s_6) + ie_{15}^{(10)} \gamma_{16} \right] \left. \right\} e^{ag_1} e^{-ks_6 g_1}, \\
m_{79} &= - \left\{ iC_{13}^{(20)} - C_{33}^{(20)} q_1 \delta_{21} - g_1' \left[ C_{44}^{(20)} (i\delta_{21} - q_1) \right] \right\} e^{-kq_1 g_1}, \\
m_{710} &= - \left\{ iC_{13}^{(20)} - C_{33}^{(20)} q_2 \delta_{22} - g_1' \left[ C_{44}^{(20)} (i\delta_{22} - q_2) \right] \right\} e^{-kq_2 g_1}, \\
m_{81} &= m_{88} = 0, \\
m_{82} &= \left\{ C_{44}^{(10)} (i\delta_{11} - s_1) + ie_{15}^{(10)} \gamma_{11} \right. \\
& \left. - g_1' \left[ iC_{11}^{(10)} - \delta_{11} s_1 C_{13}^{(10)} - \gamma_{11} s_1 e_{33}^{(10)} \right] \right\} e^{ag_1 x_1} e^{-ks_1 g_1}, \\
m_{83} &= \left\{ C_{44}^{(10)} (i\delta_{12} - s_2) + ie_{15}^{(10)} \gamma_{12} \right. \\
& \left. - g_1' \left[ iC_{11}^{(10)} - \delta_{12} s_2 C_{13}^{(10)} - \gamma_{12} s_2 e_{33}^{(10)} \right] \right\} e^{ag_1 x_1} e^{-ks_2 g_1}, \\
m_{84} &= \left\{ C_{44}^{(10)} (i\delta_{13} - s_3) + ie_{15}^{(10)} \gamma_{13} \right. \\
& \left. - g_1' \left[ iC_{11}^{(10)} - \delta_{13} s_3 C_{13}^{(10)} - \gamma_{13} s_3 e_{33}^{(10)} \right] \right\} e^{ag_1 x_1} e^{-ks_3 g_1}, \\
m_{85} &= \left\{ C_{44}^{(10)} (i\delta_{14} - s_4) + ie_{15}^{(10)} \gamma_{14} \right. \\
& \left. - g_1' \left[ iC_{11}^{(10)} - \delta_{14} s_4 C_{13}^{(10)} - \gamma_{14} s_4 e_{33}^{(10)} \right] \right\} e^{ag_1 x_1} e^{-ks_4 g_1}, \\
m_{86} &= \left\{ C_{44}^{(10)} (i\delta_{15} - s_5) + ie_{15}^{(10)} \gamma_{15} \right. \\
& \left. - g_1' \left[ iC_{11}^{(10)} - \delta_{15} s_5 C_{13}^{(10)} - \gamma_{15} s_5 e_{33}^{(10)} \right] \right\} e^{ag_1 x_1} e^{-ks_5 g_1}, \\
m_{87} &= \left\{ C_{44}^{(10)} (i\delta_{16} - s_6) + ie_{15}^{(10)} \gamma_{16} \right. \\
& \left. - g_1' \left[ iC_{11}^{(10)} - \delta_{16} s_6 C_{13}^{(10)} - \gamma_{16} s_6 e_{33}^{(10)} \right] \right\} e^{ag_1 x_1} e^{-ks_6 g_1}, \\
m_{89} &= - \left\{ C_{44}^{(20)} (i\delta_{21} - kq_1) - g_1' \left[ iC_{11}^{(20)} - C_{13}^{(20)} \delta_{21} q_1 \right] \right\} e^{-kq_1 g_1}, \\
m_{810} &= - \left\{ C_{44}^{(20)} (i\delta_{22} - kq_2) - g_1' \left[ iC_{11}^{(20)} - C_{13}^{(20)} \delta_{22} q_2 \right] \right\} e^{-kq_2 g_1}, \\
m_{91} &= m_{99} = m_{910} = 0, m_{98} = -e^{-kp g_1}, m_{92} = \gamma_{11} e^{-ks_1 g_1}, \\
m_{93} &= \gamma_{12} e^{-ks_2 g_1}, m_{94} = \gamma_{13} e^{-ks_3 g_1}, m_{94} = \gamma_{13} e^{-ks_3 g_1}, \\
m_{95} &= \gamma_{14} e^{-ks_4 g_1}, m_{96} = \gamma_{15} e^{-ks_5 g_1}, m_{97} = \gamma_{16} e^{-ks_6 g_1}, \\
m_{101} &= m_{109} = m_{1010} = m_{108} = -kpe^{-kp g_1}, \\
m_{102} &= \left\{ ie_{31}^{(10)} - e_{33}^{(10)} \delta_{11} s_1 - \kappa_{33}^{(10)} \gamma_{11} s_1 \right\} e^{ag_1} e^{-ks_1 g_1}, \\
m_{103} &= \left\{ ie_{31}^{(10)} - e_{33}^{(10)} \delta_{12} s_2 - \kappa_{33}^{(10)} \gamma_{12} s_2 \right\} e^{ag_1} e^{ks_2 g_1}, \\
m_{104} &= \left\{ ie_{31}^{(10)} - e_{33}^{(10)} \delta_{13} s_3 - \kappa_{33}^{(10)} \gamma_{13} s_3 \right\} e^{ag_1} e^{ks_3 g_1}, \\
m_{105} &= \left\{ ie_{31}^{(10)} - e_{33}^{(10)} \delta_{14} s_4 - \kappa_{33}^{(10)} \gamma_{14} s_4 \right\} e^{ag_1} e^{ks_4 g_1}, \\
m_{106} &= \left\{ ie_{31}^{(10)} - e_{33}^{(10)} \delta_{15} s_5 - \kappa_{33}^{(10)} \gamma_{15} s_5 \right\} e^{ag_1} e^{ks_5 g_1}, \\
m_{107} &= \left\{ ie_{31}^{(10)} - e_{33}^{(10)} \delta_{16} s_6 - \kappa_{33}^{(10)} \gamma_{16} s_6 \right\} e^{ag_1} e^{ks_6 g_1},
\end{aligned}$$

**Appendix H**

$$\begin{aligned}
n_{11} &= m_{12}, n_{12} = m_{13}, n_{13} = m_{14}, n_{14} = m_{15}, n_{15} = m_{16}, \\
n_{16} &= m_{17}, n_{17} = n_{18} = n_{19} = 0, n_{21} = m_{22}, n_{22} = m_{23}, \\
n_{23} &= m_{24}, n_{24} = m_{25}, n_{25} = m_{26}, n_{26} = m_{27}, \\
n_{27} &= n_{28} = n_{29} = 0, n_{31} = \gamma_{11} e^{ks_1[-h+g_2]}, \\
n_{32} &= \gamma_{12} e^{ks_2[-h+g_2]}, n_{33} = \gamma_{13} e^{ks_3[-h+g_2]}, \\
n_{34} &= \gamma_{14} e^{ks_4[-h+g_2]}, n_{35} = \gamma_{15} e^{ks_5[-h+g_2]}, \\
n_{36} &= \gamma_{16} e^{ks_6[-h+g_2]}, n_{37} = n_{38} = n_{39} = 0, \\
n_{41} &= m_{52}, n_{42} = m_{53}, n_{43} = m_{54}, n_{44} = m_{55}, n_{45} = m_{56}, \\
n_{46} &= m_{57}, n_{47} = 0, n_{48} = m_{59}, n_{49} = m_{510}, \\
n_{51} &= m_{62}, n_{52} = m_{63}, n_{53} = m_{64}, n_{54} = m_{65}, n_{55} = m_{66}, \\
n_{56} &= m_{67}, n_{57} = 0, n_{58} = m_{69}, n_{59} = m_{610}, \\
n_{61} &= m_{72}, n_{62} = m_{73}, n_{63} = m_{74}, n_{64} = m_{75}, n_{65} = m_{76}, \\
n_{66} &= m_{77}, n_{67} = 0, n_{68} = m_{79}, n_{69} = m_{710}, \\
n_{71} &= m_{82}, n_{72} = m_{83}, n_{73} = m_{84}, n_{74} = m_{85}, n_{75} = m_{86}, \\
n_{76} &= m_{87}, n_{77} = 0, n_{78} = m_{89}, n_{79} = m_{810}, \\
n_{81} &= m_{92}, n_{82} = m_{93}, n_{83} = m_{94}, n_{84} = m_{95}, n_{85} = m_{96}, \\
n_{86} &= m_{97}, n_{87} = m_{98}, n_{88} = n_{89} = 0, \\
n_{91} &= m_{102}, n_{92} = m_{103}, n_{93} = m_{104}, n_{94} = m_{105}, n_{95} = m_{106}, \\
n_{96} &= m_{107}, n_{97} = m_{108}, n_{98} = n_{99} = 0.
\end{aligned}$$